

Evaluating the Efficacy of Targeted Pesticide Applications and Machine Learning Integration for Precision Turfgrass Management

Elisabeth Clover Artemis Kitchin

Thesis submitted to the faculty of the Virginia Polytechnic Institute and State University
in partial fulfillment of the requirements for the degree of

Master of Science in Life Science
In
Plant Pathology, Physiology, and Weed Science

David S. McCall, Chair
Shawn D. Askew
Yuan Zeng

May 6th, 2025
Blacksburg, Virginia

Keywords:
Precision Agriculture
Turfgrass
Pest Mapping
Golf Courses
Targeted Pesticide Application

Copyright 2025, Elisabeth C.A. Kitchin

Evaluating the Efficacy of Targeted Pesticide Applications and Machine Learning Integration for Precision Turfgrass Management

Elisabeth Clover Artemis Kitchin

Academic Abstract

There is an increasing demand for sustainability in turfgrass pest management, emphasizing the need to reduce chemical inputs while maintaining effective pest control. Precision turfgrass management (PTM), a subset of precision agriculture, addresses these sustainability goals by tailoring management practices to the site-specific variability of the landscape. Targeted pesticide applications are a fundamental practice within PTM, involving precisely delineating pest outbreaks to create pest maps. These pest maps are then used as a guide for Global Navigation Satellite System (GNSS)-guided sprayers to apply pesticides solely to pest-affected areas as opposed to traditional broadcast pesticide applications. However, significant barriers have hindered the widespread adoption of these practices. A prominent limiting factor to the adoption of GNSS-guided sprayers is turfgrass manager's skepticism of the technology's accuracy due to a lack of documented quantifiable data demonstrating its capabilities. Additionally, the considerable labor, technical skills, and resources needed to create spatially accurate pest maps create another substantial barrier for turfgrass practitioners. An investigation into the accuracy and precision of GNSS-guided sprayers examined the influence of operational parameters such as travel speed and target size on spray deposition patterns. Fluorescent dye imaging under ultraviolet illumination, coupled with digital image analysis, quantified spray accuracy, overspray, and overlap. Results showed that the sprayer applied solution less accurately when operated at 4.8 kilometers per hour (km/h) compared to 7.2 or 9.7 km/h. Target size had no significant impact on any metric tested, indicating that targeted pesticide applications made while traveling 7.2-9.7 km/h were highly accurate, no matter the target size. An automated solution for pest mapping using machine learning was developed to identify and quantify dollar spot (*Clarireedia* spp.), a common turfgrass disease. A semantic segmentation model (DeepLabV3+) was trained on diverse images featuring various turfgrass species, disease severities, and environmental conditions. The developed model successfully automated the identification and quantification of dollar spot, offering significant improvements in efficiency, consistency, and accuracy compared to manual visual assessments. Overall, these findings demonstrate the efficacy of GNSS-guided sprayers under specific operational conditions and validate machine learning as a viable method for automating pest mapping. Future research should focus on optimizing technological and operational aspects to improve the practicality and effectiveness of precision turfgrass management.

Evaluating the Efficacy of Targeted Pesticide Applications and Machine Learning Integration for Precision Turfgrass Management

Elisabeth Clover Artemis Kitchin

General Audience Abstract

There is a growing emphasis on making turfgrass management more sustainable, especially in pest control. Traditional pest management methods often involve applying pesticides broadly across entire landscapes, which can be environmentally harmful and costly. Precision turfgrass management (PTM) addresses this issue by tailoring practices to the localized needs of the turfgrass, rather than applying uniform management across the entire system. PTM includes targeted pesticide applications, which involve creating detailed pest outbreak maps and using GNSS-guided sprayers to apply pesticides only to affected areas. Despite the potential environmental and economic benefits of targeted applications, their adoption is limited due to skepticism regarding their effectiveness and the substantial time, expertise, and resources required to create accurate pest maps. Documenting the accuracy and consistency of these sprayers and developing solutions to reduce the time and resource required for pest mapping is necessary in order to promote the widespread adoption of targeted pesticide applications. A GNSS-guided sprayer was evaluated for its accuracy and consistency when making targeted pesticide applications on turfgrass. Factors that may influence the sprayer's performance, such as the speed of travel and the target size, were assessed to measure their impact on the application accuracy. Fluorescent dye illuminated by ultraviolet (UV) lights was used to measure the sprayer deposition's proximity to the intended target and the consistency of applications across repeated trials. Applications at 4.8 km/h were significantly less accurate than those at 7.2 or 9.7 km/h. Target size had no significant impact on any metric tested, indicating that targeted pesticide applications made while traveling 7.2-9.7 km/h were highly accurate, no matter the target size. A machine learning model was trained to detect and quantify instances of dollar spot, a common turfgrass disease, across images of various turfgrass types and conditions. This model greatly reduced the effort needed for pest mapping, providing faster, more consistent, and more accurate results compared to manual inspections. Together, these efforts demonstrate that GNSS-guided sprayers can be effective when operated under optimal conditions and that automated mapping techniques using machine learning can significantly simplify and improve pest identification. Advancements in GNSS-guided sprayers and automated pest mapping will improve their practicality, encouraging broader adoption of sustainable turfgrass management practices.

Dedication

I dedicate this thesis to my family.

To my parents, Kyle and Helena, for their lifetime of support and endless love. You have given everything to support me in the pursuit of my dreams. Words cannot capture the immense gratitude and the love I have for you both.

To my sisters, Emma and Eden. You are my biggest cheerleaders (and the funniest people I know). Being your sister is the greatest privilege of my life.

And to my incredible fiancé, Henry. You are my inspiration, my collaborator, and my best friend. I do not fear the future because I have you by my side.

Acknowledgements

I want to express my sincerest appreciation to my principal advisor, Dr. David McCall, for going above and beyond as a mentor and researcher. None of my work would be possible without your abundance of encouragement, support, and patience.

I'm also incredibly grateful to my co-advisor, Dr. Shawn Askew, for his invaluable guidance and assistance with these projects. I would also like to extend my gratitude to my committee member, Dr. Yuan Zeng, for her support and assistance throughout my time at Virginia Tech.

Special thanks to the members of the McCall lab, former and current, who selflessly gave their time and energy to help with my research, and who I am lucky to consider friends; Kevin Hensler, Ava Veith, Travis Roberson, Aaron Tucker, and Caleb Henderson.

I'd also like to thank Dr. Michael Goatley, Dr. Dan Sandor, Mrs. Whitnee Askew, and Mr. John Hinson, for their kindness and help throughout the course of my master's degree. It truly does take a village, and I am forever grateful for the abundance of support I have received from the Virginia Tech Turf Team.

Thank you to the Virginia Turfgrass Foundation for their generous and continued support of myself and my research.

Table of Contents

TITLE PAGE	I
ACADEMIC ABSTRACT	II
GENERAL AUDIENCE ABSTRACT.....	III
DEDICATION	IV
ACKNOWLEDGEMENTS	V
TABLE OF CONTENTS	VI
LIST OF TABLES	VII
LIST OF FIGURES	VIII
CHAPTER 1: LITERATURE REVIEW	1
INTRODUCTION	1
PRECISION TURFGRASS MANAGEMENT	3
TARGETED PESTICIDE APPLICATIONS	4
PEST MAPPING	6
MACHINE LEARNING.....	7
BIBLIOGRAPHY	9
CHAPTER 2: EVALUATING FACTORS INFLUENCING THE ACCURACY AND PRECISION OF TARGETED PESTICIDE APPLICATIONS ON TURFGRASS USING A GNSS-GUIDED SPRAYER	15
ABSTRACT	15
INTRODUCTION.....	16
MATERIALS AND METHODS.....	19
RESULTS	26
DISCUSSION	30
BIBLIOGRAPHY	33
CHAPTER 3: LEVERAGING DEEP LEARNING FOR DOLLAR SPOT DETECTION AND QUANTIFICATION IN TURFGRASS	36
ABSTRACT	36
INTRODUCTION.....	37
MATERIALS AND METHODS.....	41
RESULTS	52
DISCUSSION	53
BIBLIOGRAPHY	57

List of Tables

Chapter II. Evaluating Factors Influencing the Accuracy and Precision of Targeted Pesticide Applications on Turfgrass using a GNSS-Guided Sprayer

Table 1. Analysis of variance (ANOVA) results evaluating the significance ($P < 0.05$) of the main effects of travel speed, target size, trial run, and their interactions on % overlap, offset distance, and overspray area. Significant effects are indicated in bold.

Table 2. Main effect of sprayer operational speed on percentage overlap, offset distance, and overspray area of precision spray averaged over three target sizes and three trials. Means not connected by the same letter are significantly different at $P < 0.05$.

Table 3. Interaction of speed by target size on overspray area of precision spray averaged over three trials. Means not connected by the same letter are significantly different at $P < 0.05$.

Chapter III. Leveraging Deep Learning for Dollar Spot Detection and Quantification in Turfgrass

Table 1. Specifications of computing environment used in this study for deep learning of dollar spot detection.

Table 2. Performance metrics across varying levels of disease prevalence.

List of Figures

Chapter II. Evaluating Factors Influencing the Accuracy and Precision of Targeted Pesticide Applications on Turfgrass using a GNSS-Guided Sprayer

Figure 1. ArcGIS Pro shapefile map of trial area depicting targets randomly placed throughout each travel speed strip.

Figure 2. The distribution of spray centroids relative to the intended target center, represented by an orange X, with maroon dots indicating actual spray centroid locations.

Chapter III. Leveraging Deep Learning for Dollar Spot Detection and Quantification in Turfgrass

Figure 1. A visualization of computer vision tasks categorizing dollar spot on turfgrass. For the image classification task, the image is classified as containing dollar spot since it is the prevailing disease afflicting the turfgrass. For the object detection task, bounding boxes are drawn around each instance of dollar spot. For the semantic segmentation task, the model predicts the binary probability that each pixel represents dollar spot, creating masks that identify affected areas.

Figure 2. Data preprocessing and augmentation from left to right: every instance of dollar spot from the original field image of dollar spot is labeled by hand to create the mask. The mask is then sliced into 256×256 pixel tiles and a mirror image is generated. The tiles from the image and its mirror are both added to the dataset, and any tiles with more than 20% disease are duplicated in the final dataset.

Figure 3. Predicted dollar spot masks from a creeping bentgrass fairway using varying confidence thresholds. Columns from left to right represent the original image, the predicted probability, the predicted mask, and the ground truth image used for training. Rows represent dollar spot predictions at confidence thresholds of 10%, 90%, and 99%.

Chapter 1: Literature Review

Introduction to Turfgrass & Turfgrass Management

Turfgrasses are a small subsection of grass species that are recognized for their ability to form a low-growing, densely-knit ground cover, while withstanding continuous stress from defoliation and traffic (Christians et al., 2016). In the United States, roughly 163,800 km² is covered by turfgrass systems, including both maintained and non-maintained, no-input systems (Milesi et al., 2005). The turfgrass industry has been estimated to employ over 800,000 individuals and generate roughly \$60 billion in the United States (Hall et al., 2006; Haydu et al., 2006). In addition to economic value, turfgrasses provide a wide variety of economic, societal, and environmental benefits (Beard & Green, 1994; Braun et al., 2024). Environmental benefits, also described as ecosystem services, of turfgrass include urban cooling through evapotranspiration (Monteiro, 2017), soil stabilization and remediation (Chang et al., 2021; Easton & Petrovic, 2004), groundwater filtration and runoff reduction (Steinke et al., 2009; Gross et al., 1991), and carbon sequestration (Braun & Bremer, 2019; Phillips et al., 2023; Singh et al., 2019). Societal benefits of turfgrass can range from improving human mental health (Bratman et al., 2019; Van den Berg et al., 2015) to promoting physical health and wellness (Hassan & Deshun, 2024; Jia et al., 2021).

To maintain the diverse range of benefits that turfgrass systems provide, varying degrees of management and regular maintenance are often required. Each turfgrass species has specific cultural requirements, with some persisting with little to no inputs, whereas others require more intensive management practices to maintain their expected

performance. In addition to maintaining the health of the turfgrass, there are also high expectations to maintain the aesthetics of some managed turfgrass systems (Herzog & Chernick, 2000; Jung & Chung, 2024). These demands necessitate dedicated management plans to ensure the consistent health and performance of the turfgrass surface, in addition to maintaining its aesthetic qualities. However, these dedicated management plans often increase the amount of water, fertilizer, and pesticides used on golf courses (Carlson et al., 2022).

Diseases pose a formidable challenge to turfgrass management, with roughly \$150 million spent annually on fungicides in the United States (Tredway et al., 2022). Turfgrass disease management is multifaceted and can involve planting genetically resistant turfgrass varieties, modifying the environment to limit the spread of disease, using appropriate cultural practices, and applying biological or chemical treatments (Tredway et al., 2022). Although synthetic chemical pesticides have well-documented efficacy and target-specificity, pesticides can have unpredictable nontarget effects (Smiley, 1981). Nontarget runoff from pesticides applied to golf courses can cause waterway contamination and toxicity to aquatic organisms (Baris et al., 2010; Haith & Rossi, 2003; Metcalfe et al., 2008). Continuous pesticide usage can potentially be hazardous to the health of golf course workers (Knopper & Lean, 2004; Kross et al., 1996). Pesticides can increase the risk of arsenic contamination in groundwater (Cai et al., 2002) and may negatively affect beneficial soilborne organisms and invertebrates (Gunstone et al., 2021). Due to these risks, there are increasing calls from the public to reduce pesticide usage on turfgrass (Beyond Pesticides, 2021; Garris, 2018). Reducing pesticide use, particularly fungicides, can mitigate risks associated with pesticides on golf

courses (Bekken et al., 2021). Here emerges a complex issue for turfgrass managers: how to reconcile the demand for high-quality, attractive turfgrass with rising calls to reduce chemical inputs (Held & Potter, 2012).

Precision Turfgrass Management

Precision turfgrass management (PTM) has emerged as a promising solution to this issue (Braun et al., 2023; Carlson et al., 2022). A subset of precision agriculture, PTM describes a range of methods and management practices used to improve input efficiency while maintaining turfgrass health and aesthetic quality (Carlson et al., 2022). Turfgrass systems especially benefit from precision management practices due to the inherent spatial variability and site-specific input requirements of golf courses, athletic fields, landscaping, and utility areas (Bell et al., 2013). In practice, precision turfgrass management involves establishing site-specific management zones by identifying spatial variability within the turfgrass system and then directing inputs such as fertilizers, irrigation, or pesticides only where they are needed (Braun et al., 2023; Carlson et al., 2022; Carrow et al., 2010; Krum et al., 2010). Management zones and spatial variability across the turfgrass system are most often distinguished and delineated using Global Navigation Satellite Systems (GNSS) and Geographic Information System (GIS) technology (Krum et al., 2010).

GNSS technology, the most commonly used positioning system in precision agriculture applications, refers to a collection of satellites used to determine a receiver's precise location (Perez-Ruiz et al., 2012). GNSS receivers play a foundational role in precision agriculture applications, as the highly specific locational data they provide is

essential for site-specific management. Real-Time Kinematic (RTK) systems improve Global Navigation Satellite System (GNSS) positioning by correcting satellite data errors in real time, achieving centimeter-level accuracy (average error < 2 cm) (Perez-Ruiz et al., 2012; Hou et al., 2023). Geographic Information System (GIS) software uses this precise georeferenced data to create detailed spatial maps that identify variability within turfgrass systems (Braun et al., 2023; Krum et al., 2010). In turfgrass research, combined GNSS and GIS technologies have been employed to study the spatial aggregation and etiology of diseases like dollar spot (*Clariireedia* spp.) and large patch (*Rhizoctonia* spp.) (Horvath et al., 2007; Spurlock & Milus, 2009). Henry et al. (2009) employed GNSS technology to study the environmental conditions and cultural management practices associated with bahiagrass (*Paspalum notatus* Fluegge) and dallisgrass (*Paspalum dilatatum* Poir.).

Targeted Pesticide Applications

Site-specific pesticide application, commonly referred to as Variable Rate Pesticide Application (VRPA), uses technology to adjust application rates based on pest presence and severity while avoiding treatment in non-target areas (Karkee et al., 2013). One of the most common methods of VRPA is the map-based approach, where a sprayer equipped with a GNSS receiver identifies its field position and adjusts the application rate based on a prescription map as it moves through the field (Balafoutis et al., 2017). Map-based approaches often rely on modulated spraying-nozzle control (MSNC) systems combined with automatic section control (ASC), to enable precise, site-specific application adjustments. These systems enable individual nozzle control, adjusting flow

rates in real time based on field location and the presence of pests. As the sprayer navigates according to the prescription map, MSNC systems are able to shut off single nozzles or nozzle sections over areas already treated or free of pests, applying pesticides only where needed (Grisso et al., 2011).

Map-based targeted pesticide applications with GNSS-guided sprayers provide effective, site-specific pest control while significantly reducing input requirements (Luck et al., 2010; Sharda et al., 2013). When using UAV sprayers, site-specific herbicide applications reduced inputs by 20-60% compared to full-coverage applications (Hunter III et al., 2020). A study by Booth et al. found that, when treating spring dead spot (*Ophiosphaerella* spp.), targeted, site-specific fungicide applications used 50-60% less fungicides while maintaining similar levels of disease suppression as traditional full-coverage applications (Booth et al., 2021). However, Booth et al. (2021) note that despite the benefits of targeted pesticide applications, more research is necessary to improve efficacy when using GPS-guided sprayers with individual nozzle control, and further refinement for site-specific applications is necessary. Sharda et al. (2013) note that off-rate errors in GPS-guided applications are significantly affected by automatic nozzle control and variations in ground speed. Their findings show that deceleration with MSNC turning sections off led to over-application, while acceleration with sections turning on often resulted in under-application. The study suggests that further research is needed to optimize the efficacy of map-based targeted VRPA using GPS sprayers, particularly in understanding how factors such as ground speed and target size influence the precision and accuracy of applications. Despite the promising potential of this technology, many industry practitioners do not have a thorough understanding of the benefits and

applications of these advancements, thus creating a need for evidentiary support of the potential positive impacts (McBratney et al., 2005); Kutter et al., 2011).

Pest Mapping

A key component of map-based VRPA is the maps themselves, which are made by identifying and segmenting instances of pests and their spatial distribution. These pest maps enable targeted pesticide applications and document disease growth and development spatially and temporally (Bell et al., 2013; Delgado et al., 2008; Hutchens et al., 2024). The creation of pest maps has historically relied on physically scouting for and identifying the presence of pests. These manual assessments rely on visual identification and quantification, which can be subject to variation among different assessors (Bock et al., 2020; Nutter Jr et al., 1993; Schwanck & Del Ponte, 2014; Shahi et al., 2023).

Additionally, the process of creating pest maps can be laborious and time-consuming, especially when documenting pests over a large area of land. Digital image analysis (DIA) has been used to expedite this process, analyzing images and providing accurate estimations of pest incidence and severity, allowing for a reliable, consistent, and autonomous method of pest mapping (Karcher & Richardson, 2013; Sykes et al., 2017). Applications of DIA for pest mapping are limited, however, by its inability to differentiate between different diseases, weeds, and abiotic stresses. This hinders the use of DIA when analyzing turfgrass images with more than one pest or abiotic issue present (Karcher & Richardson, 2013).

Recent technological advancements, such as the development of Unmanned Aerial Vehicles (UAVs), the Internet of Things (IoT), and software programs, have

allowed for the adoption of semi-autonomous, rapid, highly accurate pest detection and mapping in agriculture (Shahi et al., 2023). A Python-based script was developed by Henderson et al. (2021) to automate the mapping of spring dead spot using UAV imagery. This script greatly improved image processing speeds, though it still required manual intervention in the processing procedure (Henderson, 2021). A solution to these manual intervention requirements is provided in the form of machine learning, which allows for quick and accurate analysis of imagery without cumbersome labor requirements and has proven to be an incredibly efficient method for pest mapping in agricultural settings (Shahi et al., 2023).

Machine Learning for Turfgrass Pest Management

Machine learning has become increasingly prominent in agricultural applications in recent years. Though use cases vary, machine learning models typically involve one or more of four main tasks: identification, classification, quantification, and prediction. Identification begins with detecting specific targets such as distinguishing plant types or locating disease presence. Classification groups visual data into specific categories, such as different stress levels or types of weeds and diseases. Quantification measures the extent of these phenomena, such as estimating coverage area or incidence rates, which is crucial for assessing weed invasions or disease spread across a field. Finally, prediction allows for anticipating these issues before visible symptoms arise, supporting proactive, cost-effective management in precision agriculture (Singh et al., 2018). For autonomous pest identification purposes, machine learning models with identification, classification, and quantification capabilities are most applicable. Deep learning has been used to

autonomously identify various weeds in a range of turfgrass systems for precision herbicide applications (Jin et al., 2022; Joseph et al., 2024; J. Yu et al., 2020; J. Yu, Schumann, et al., 2019; J. Yu, Sharpe, et al., 2019). Other aspects of turfgrass health, such as visual quality and color (Ding et al., 2016) and clipping yields (Zhou & Soldat, 2021, 2022), have been successfully analyzed using deep learning techniques. Despite successful applications in crops such as cereal grains (Waldamichael et al., 2022), tomatoes (Durmus et al., 2017), and soybeans (M. Yu et al., 2022), machine learning for disease detection on turfgrass remains unexplored. The ability of deep learning models to overcome technical limitations in performing autonomous disease detection makes them a promising candidate to assist in the identification of turfgrass pests (Boulent et al., 2019).

Bibliography

1. Balafoutis, A., Beck, B., Fountas, S., Vangeyte, J., Wal, T. V., Soto, I., Gómez-Barbero, M., Barnes, A., & Eory, V. (2017). Precision Agriculture Technologies Positively Contributing to GHG Emissions Mitigation, Farm Productivity, and Economics. *Sustainability*, 9(8), Article 1339. <https://doi.org/10.3390/su9081339>
2. Balogh, J. C., & Anderson, J. L. (2020). Environmental Impacts of Turfgrass Pesticides. *Golf Course Management & Construction*, 221–353.
3. Baris, R. D., Cohen, S. Z., Barnes, N. L., Lam, J., & Ma, Q. (2010). Quantitative Analysis of Over 20 Years of Golf Course Monitoring Studies. *Environmental Toxicology and Chemistry*, 29(6), 1224–1236. <https://doi.org/10.1002/etc.185>
4. Beard, J. B., & Green, R. L. (1994). The Role of Turfgrasses in Environmental Protection and Their Benefits to Humans. *Journal of Environmental Quality*, 23(3), 452–460. <https://doi.org/10.2134/jeq1994.00472425002300030007x>
5. Bekken, M. A., Schimenti, C. S., Soldat, D. J., & Rossi, F. S. (2021). A Novel Framework for Estimating and Analyzing Pesticide Risk on Golf Courses. *Science of the Total Environment*, 783, <https://doi.org/10.1016/j.scitotenv.2021.146840>
6. Bell, G. E., Kruse, J. K., & Krum, J. M. (2013). The Evolution of Spectral Sensing and Advances in Precision Turfgrass Management. In *Turfgrass: Biology, Use, and Management* (Vol. 56, pp. 1151–1188).
7. Beyond Pesticides. (2021). *Golf, Pesticides, and Organic Practices*. Beyond Pesticides. Environmental Protection, 11, 16.
8. Bock, C. H., Barbedo, J. G., Del Ponte, E. M., Bohnenkamp, D., & Mahlein, A.-K. (2020). From Visual Estimates to Fully Automated Sensor-Based Measurements of Plant Disease Severity: Status and Challenges for Improving Accuracy. *Phytopathology Research*, 2, 1–30. <https://doi.org/10.1186/s42483-020-00049-8>
9. Booth, J. C., Sullivan, D., Askew, S. A., Kochersberger, K., & McCall, D. S. (2021). Investigating Targeted Spring Dead Spot Management Via Aerial Mapping and Precision-Guided Fungicide Applications. *Crop Science*, 61(5), 3134–3144. <https://doi.org/10.1002/csc2.20623>
10. Boulent, J., Foucher, S., Théau, J., & St-Charles, P.-L. (2019). Convolutional Neural Networks for the Automatic Identification of Plant Diseases. *Frontiers in Plant Science*, 10, 941. <https://doi.org/10.3389/fpls.2019.00941>
11. Braun, R. C., Mandal, P., Nwachukwu, E., & Stanton, A. (2024). The Role of Turfgrasses in Environmental Protection and Their Benefits to Humans: Thirty Years Later. *Crop Science*. <https://doi.org/10.1002/csc2.21383>
12. Braun, R. C., Straw, C. M., Soldat, D. J., Bekken, M. A., Patton, A. J., Lonsdorf, E. V., & Horgan, B. P. (2023). Strategies for Reducing Inputs and Emissions in

- Turfgrass Systems. *Crop, Forage & Turfgrass Management*, 9(1), e20218. <https://doi.org/10.1002/cft2.20218>
13. Cai, Y., Cabrera, J. C., Georgiadis, M., & Jayachandran, K. (2002). Assessment of Arsenic Mobility in the Soils of Some Golf Courses in South Florida. *Science of the Total Environment*, 291(1–3), 123–134. [https://doi.org/10.1016/S0048-9697\(01\)01081-6](https://doi.org/10.1016/S0048-9697(01)01081-6)
 14. Carlson, M. G., Gaussoin, R. E., & Puntel, L. A. (2022). A Review of Precision Management for Golf Course Turfgrass. *Crop, Forage & Turfgrass Management*, 8(2), e20183. <https://doi.org/10.1002/cft2.20183>
 15. Carrow, R. N., Krum, J. M., Flitcroft, I., & Cline, V. (2010). Precision Turfgrass Management: Challenges and Field Applications for Mapping Turfgrass Soil and Stress. *Precision Agriculture*, 11(2), 115–134. <https://doi.org/10.1007/s11119-009-9136-y>
 16. Christians, N. E., Patton, A. J., & Law, Q. D. (2016). *Fundamentals of Turfgrass Management* (5th ed.). John Wiley & Sons.
 17. Clarke, B. B., Vincelli, P., Koch, P., & Chou, M.-Y. (2020). *Chemical Control of Turfgrass Diseases 2024*.
 18. Delgado, J. A., Berry, J. K., & Khosla, R. (2008). New Advances and Practices for Precision Conservation (pp. 21–23).
 19. Ding, K., Raheja, A., Bhandari, S., & Green, R. L. (2016). Application of Machine Learning for the Evaluation of Turfgrass Plots Using Aerial Images. In *Autonomous Air and Ground Sensing Systems for Agricultural Optimization and Phenotyping II* (Vol. 9866, pp. 84–96). <https://doi.org/10.1117/12.2228695>
 20. Durmuş, H., Güneş, E. O., & Kırıcı, M. (2017). Disease Detection on the Leaves of Tomato Plants by Using Deep Learning. In *2017 IEEE 25th Signal Processing and Communications Applications Conference* (pp. 1–5). DOI: 10.1109/Agro-Geoinformatics.2017.8047016
 21. Easton, Z. M., & Petrovic, A. M. (2004). Fertilizer Source Effect on Ground and Surface Water Quality in Drainage From Turfgrass. *Journal of Environmental Quality*, 33(2), 645–655. <https://doi.org/10.2134/jeq2004.6450>
 22. Feng, M., Schrlau, J. E., Snyder, R., Snyder, G. H., Chen, M., Cisar, J. L., & Cai, Y. (2005). Arsenic Transport and Transformation Associated With MSMA Application on a Golf Course Green. *Journal of Agricultural and Food Chemistry*, 53(9), 3556–3562. DOI: 10.1021/jf047908j
 23. Garris, W. (2018). Could the Golf Course Green Be Poisoning You and Your Child? *Medium*. <https://medium.com/@wgarris/could-the-golf-course-green-be-poisoning-you-and-your-child-5646511965c7>
 24. Grisso, R. D., Alley, M. M., Thomason, W. E., Holshouser, D. L., & Roberson, G. T. (2011). *Precision Farming Tools: Variable-Rate Application* (Publication 442-502). Virginia Cooperative Extension.

25. Gunstone, T., Cornelisse, T., Klein, K., Dubey, A., & Donley, N. (2021). Pesticides and Soil Invertebrates: A Hazard Assessment. *Frontiers in Environmental Science*, 9, 643847. <https://doi.org/10.3389/fenvs.2021.643847>
26. Haith, D. A., & Rossi, F. S. (2003). Risk Assessment of Pesticide Runoff From Turf. *Journal of Environmental Quality*, 32(2), 447–455. <https://doi.org/10.2134/jeq2003.4470>
27. Hassan, A., & Deshun, Z. (2024). Psychophysiological Impact of Touching Landscape Grass Among Older Adults. *Journal of Urban Health*, 1–12. <https://doi.org/10.1007/s11524-024-00875-7>
28. Held, D. W., & Potter, D. A. (2012). Prospects for Managing Turfgrass Pests With Reduced Chemical Inputs. *Annual Review of Entomology*, 57, 329–354. <https://doi.org/10.1146/annurev-ento-120710-100542>
29. Henderson, C. A. (2021). Identification of disease stress in turfgrass canopies using thermal imagery and automated aerial image analysis (Master's Thesis, Virginia Tech).
30. Henry, G. M., Burton, M. G., & Yelverton, F. H. (2009). Heterogeneous Distribution of Weedy *Paspalum* Species and Edaphic Variables in Turfgrass. *HortScience*, 44(2), 447–451. <https://doi.org/10.21273/HORTSCI.44.2.447>
31. Herzog, T. R., & Chernick, K. K. (2000). Tranquility and Danger in Urban and Natural Settings. *Journal of Environmental Psychology*, 20(1), 29–39. <https://doi.org/10.1006/jevps.1999.0151>
32. Horvath, B., Kravchenko, A., Robertson, G., & Vargas, J., Jr. (2007). Geostatistical Analysis of Dollar Spot Epidemics Occurring on a Mixed Sward of Creeping Bentgrass and Annual Bluegrass. *Crop Science*, 47(3), 1206–1216. <https://doi.org/10.2135/cropsci2006.09.0565>
33. Hou, P., Zha, J., Liu, T., & Zhang, B. (2023). Recent Advances and Perspectives in GNSS PPP-RTK. *Measurement Science and Technology*, 34(5), 051002. DOI 10.1088/1361-6501/acb78c
34. Hunter, J. E., III, Gannon, T. W., Richardson, R. J., Yelverton, F. H., & Leon, R. G. (2020). Integration of Remote-Weed Mapping and an Autonomous Spraying Unmanned Aerial Vehicle for Site-Specific Weed Management. *Pest Management Science*, 76(4), 1386–1392. <https://doi.org/10.1002/ps.5651>
35. Hutchens, W. J., Henderson, C., Straw, C., Goatley, J., Kerns, J., Nita, M., Sullivan, D., & McCall, D. S. (2024). Environmental and Edaphic Factors That Influence Spring Dead Spot Epidemics. *Phytopathology*, 114(1), 155–163. <https://doi.org/10.1094/PHYTO-10-22-0398-R>
36. Jia, P., Cao, X., Yang, H., Dai, S., He, P., Huang, G., Wu, T., & Wang, Y. (2021). Green Space Access in the Neighbourhood and Childhood Obesity. *Obesity Reviews*, 22, e13100. <https://doi-org.ezproxy.lib.vt.edu/10.1111/obr.13100>

37. Jin, X., Bagavathiannan, M., Maity, A., Chen, Y., & Yu, J. (2022). Deep Learning for Detecting Herbicide Weed Control Spectrum in Turfgrass. *Plant Methods*, *18*, 94. <https://doi.org/10.1186/s13007-022-00929-4>
38. Joseph, M. M., Gawron, K. A., Zhao, C., MacDonald, G. E., Schumann, A. W., Boyd, N. S., & Petelewicz, P. (2024). Evaluation of Segmentation and Semi-Supervised Learning for Spotted Spurge Recognition in Bermudagrass Turf. *International Turfgrass Society Research Journal*. <https://doi-org.ezproxy.lib.vt.edu/10.1002/its2.152>
39. Karcher, D. E., & Richardson, M. D. (2013). Digital Image Analysis in Turfgrass Research. In *Turfgrass: Biology, Use, and Management* (Vol. 56, pp. 1133–1149).
40. Karkee, M., Steward, B., & Kruckeberg, J. (2013). Automation of Pesticide Application Systems. In *Agricultural Automation: Fundamentals and Practices* (pp. 263–278).
41. Kitchin, E. C., Sneed, H. J., & McCall, D. S. (2024). Leveraging Deep Learning for Dollar Spot Detection and Quantification in Turfgrass. *Crop Science*. <https://doi.org/10.1002/csc2.21329>
42. Knopper, L. D., & Lean, D. R. (2004). Carcinogenic and Genotoxic Potential of Turf Pesticides Commonly Used on Golf Courses. *Journal of Toxicology and Environmental Health, Part B*, *7*(4), 267–279. <https://doi.org/10.1080/10937400490452697>
43. Kross, B. C., Burmeister, L. F., Ogilvie, L. K., Fuortes, L. J., & Fu, C. M. (1996). Proportionate Mortality Study of Golf Course Superintendents. *American Journal of Industrial Medicine*, *29*(5), 501–506.
44. Krum, J. M., Carrow, R. N., & Karnok, K. (2010). Spatial Mapping of Complex Turfgrass Sites: Site-Specific Management Units and Protocols. *Crop Science*, *50*(1), 301–315. <https://doi.org/10.2135/cropsci2009.04.0173>
45. Kutter, T., Tiemann, S., Siebert, R., & Fountas, S. (2011). The Role of Communication and Co-Operation in the Adoption of Precision Farming. *Precision Agriculture*, *12*(1), 2–17. <https://doi.org/10.1007/s11119-009-9150-0>
46. Luck, J., Zandonadi, R., Luck, B., & Shearer, S. (2010). Reducing Pesticide Over-Application With Map-Based Automatic Boom Section Control on Agricultural Sprayers. *Transactions of the ASABE*, *53*(3), 685–690. DOI: 10.13031/2013.30060
47. McBratney, A., Whelan, B., Ancev, T., & Bouma, J. (2005). Future Directions of Precision Agriculture. *Precision Agriculture*, *6*(1), 7–23. <https://doi.org/10.1007/s11119-005-0681-8>
48. Metcalfe, T. L., Dillon, P. J., & Metcalfe, C. D. (2008). Detecting the Transport of Toxic Pesticides From Golf Courses Into Watersheds in the Precambrian Shield

- Region of Ontario, Canada. *Environmental Toxicology and Chemistry*, 27(4), 811–818. <https://doi.org/10.1897/07-216.1>
49. Milesi, C., Running, S. W., Elvidge, C. D., Dietz, J. B., Tuttle, B. T., & Nemani, R. R. (2005). Mapping and Modeling the Biogeochemical Cycling of Turf Grasses in the United States. *Environmental Management*, 36, 426–438. <https://doi.org/10.1007/s00267-004-0316-2>
 50. Monteiro, J. A. (2017). Ecosystem Services From Turfgrass Landscapes. *Urban Forestry & Urban Greening*, 26, 151–157. <https://doi.org/10.1016/j.ufug.2017.04.001>
 51. Nutter, F., Jr., Gleason, M., Jenco, J., & Christians, N. (1993). Assessing the Accuracy, Intra-Rater Repeatability, and Inter-Rater Reliability of Disease Assessment Systems. *Phytopathology*, 83(8), 806–812.
 52. Perez-Ruiz, M., & Upadhyaya, S. K. (2012). GNSS in Precision Agricultural Operations. In *New Approach of Indoor and Outdoor Localization Systems* (pp. 3–26).
 53. Schwanck, A. A., & Del Ponte, E. M. (2014). Accuracy and Reliability of Severity Estimates Using Linear or Logarithmic Disease Diagram Sets in True Colour or Black and White: A Study Case for Rice Brown Spot. *Journal of Phytopathology*, 162(10), 670–682. <https://doi.org/10.1111/jph.12246>
 54. Shahi, T. B., Xu, C.-Y., Neupane, A., & Guo, W. (2023). Recent Advances in Crop Disease Detection Using UAV and Deep Learning Techniques. *Remote Sensing*, 15(9), 2450. <https://doi.org/10.3390/rs15092450>
 55. Sharda, A., Luck, J. D., Fulton, J. P., McDonald, T. P., & Shearer, S. A. (2013). Field Application Uniformity and Accuracy of Two Rate Control Systems With Automatic Section Capabilities on Agricultural Sprayers. *Precision Agriculture*, 14, 307–322. <https://doi.org/10.1007/s11119-012-9296-z>
 56. Singh, A. K., Ganapathysubramanian, B., Sarkar, S., & Singh, A. (2018). Deep Learning for Plant Stress Phenotyping: Trends and Future Perspectives. *Trends in Plant Science*, 23(10), 883–898. <https://doi.org/10.1016/j.tplants.2018.07.004>
 57. Smiley, R. W. (1981). Non-Target Effects of Pesticides on Turf Grasses. *Plant Disease*, 65, 17–23.
 58. Spurlock, T., & Milus, E. (2009). Spatial and Temporal Occurrence of Large Patch Disease in Northwest Arkansas. *Phytopathology*, 99(6), S123.
 59. Sykes, V. R., Horvath, B. J., Warnke, S. E., Askew, S. D., Baudoin, A. B., & Goatley, J. M. (2017). Comparing Digital and Visual Evaluations for Accuracy and Precision in Estimating Tall Fescue Brown Patch Severity. *Crop Science*, 57(6), 3303–3309. <https://doi.org/10.2135/cropsci2016.08.0699>
 60. Tredway, L. P., Clarke, B. B., Kerns, J. P., & Tomaso-Peterson, M. (Eds.). (2022). *Compendium of Turfgrass Diseases* (4th ed.). The American Phytopathological Society.

61. Waldamichael, F. G., Debelee, T. G., Schwenker, F., Ayano, Y. M., & Kebede, S. R. (2022). Machine Learning in Cereal Crops Disease Detection: A Review. *Algorithms*, 15(3), 75. <https://doi.org/10.3390/a15030075>
62. Yu, J., Schumann, A. W., Cao, Z., Sharpe, S. M., & Boyd, N. S. (2019). Weed Detection in Perennial Ryegrass With Deep Learning Convolutional Neural Network. *Frontiers in Plant Science*, 10, 1422. <https://doi.org/10.3389/fpls.2019.01422>
63. Yu, J., Schumann, A. W., Sharpe, S. M., Li, X., & Boyd, N. S. (2020). Detection of Grassy Weeds in Bermudagrass With Deep Convolutional Neural Networks. *Weed Science*, 68(5), 545–552. DOI:10.1017/wsc.2020.46
64. Yu, J., Sharpe, S. M., Schumann, A. W., & Boyd, N. S. (2019a). Deep Learning for Image-Based Weed Detection in Turfgrass. *European Journal of Agronomy*, 104, 78–84. <https://doi.org/10.1016/j.eja.2019.01.004>
65. Yu, J., Sharpe, S. M., Schumann, A. W., & Boyd, N. S. (2019b). Detection of Broadleaf Weeds Growing in Turfgrass With Convolutional Neural Networks. *Pest Management Science*, 75(8), 2211–2218. DOI:10.1002/ps.5349
66. Yu, M., Ma, X., Guan, H., Liu, M., & Zhang, T. (2022). A Recognition Method of Soybean Leaf Diseases Based on an Improved Deep Learning Model. *Frontiers in Plant Science*, 13, 878834. <https://doi.org/10.3389/fpls.2022.878834>
67. Zhou, Q., & Soldat, D. J. (2022). Corrigendum: Creeping Bentgrass Yield Prediction With Machine Learning Models. *Frontiers in Plant Science*, 12. <https://doi.org/10.3389/fpls.2021.749854>

Chapter 2: Evaluating Factors Influencing the Accuracy and Precision of Targeted Pesticide Applications on Turfgrass using a GNSS-Guided Sprayer

Abstract:

Managed turfgrass systems such as golf courses and athletic fields provide essential environmental and recreational benefits but rely heavily on pesticide applications that pose environmental and economic concerns. Precision turfgrass management (PTM), utilizing global navigation satellite system (GNSS)-guided sprayers, offers a sustainable solution by enabling site-specific applications that significantly reduce chemical inputs, cost, and environmental impact. Despite their potential, limited quantitative data on the accuracy and precision of GNSS-guided sprayers have restricted widespread adoption. This study quantitatively assessed the accuracy (offset distance and percent overlap) and precision (consistency of applications) of GNSS-guided sprayer pesticide applications on a golf course fairway, considering operational parameters of travel speed (4.8, 7.2, and 9.7 km/h) and target size (0.5, 1, and 2 m). The trial employed a randomized complete block design, where target locations were accurately mapped using real-time kinematic (RTK) GNSS receivers and sprayed with fluorescent dye. Application patterns were captured by drone-based UV imaging and analyzed for offset distances, overlap percentages, and overspray areas. Results demonstrated that sprayer speed significantly influenced accuracy, with speeds of 7.2 and 9.7 km/h achieving greater overlap and lower offset distances compared to 4.8 km/h. Overspray area increased with higher travel speeds and larger target sizes, suggesting the need for operational adjustments at faster speeds. Target size alone did not significantly impact accuracy or precision, highlighting the technology's versatility across different target scales. These findings provide critical quantitative evidence of GNSS-guided sprayer effectiveness, addressing industry adoption barriers related to accuracy and efficacy concerns. Further research across various environmental conditions and equipment types is essential for broader implementation of targeted pesticide applications within PTM.

Introduction

Managed turfgrass systems, including golf courses, athletic fields, and parks, enhance urban environments by providing safe recreational spaces, mitigating erosion, moderating temperatures, and enriching landscape aesthetics (Beard & Green, 1994; Braun et al., 2024). Effective pest management is crucial for sustaining these benefits, and conventional practices have relied on chemical pesticides. Although effective in many cases, this reliance has raised concerns regarding environmental sustainability. Pesticide runoff from golf courses can degrade water quality and harm non-target organisms, including beneficial insects and pollinators (Haith, 2010; Gels et al., 2002). Moreover, blanket pesticide applications across large areas often result in chemical overuse, wasted resources, and elevated maintenance costs (Luck et al., 2010). As criticism of traditional pest management practices rises, there is increasing emphasis on adopting sustainable technologies for pest management (Braun et al., 2023).

Precision turfgrass management (PTM) is a subset of precision agriculture (PA) that enhances turfgrass management practices by tailoring site-specific applications to the natural variability of the turfgrass landscape (Bell et al., 2013; Carrow et al., 2010; Krum et al., 2010). PTM incorporates technologies such as global navigation satellite systems (GNSS) and geographic information systems (GIS) to precisely delineate areas that require intervention and directs management practices and input applications accordingly (Straw et al., 2020; Krum et al., 2010). GNSS-guided sprayers play a key role in site-specific management, specifically in applying inputs only where they are required, which significantly reduces waste, cost, and environmental impact (Carlson et al., 2022; Carrow et al., 2010). Equipped with individual nozzle control, GNSS-guided sprayers can apply

inputs within a predetermined boundary without manual intervention to turn the boom on and off (Braun et al., 2023). The adoption of these sprayers addresses two central goals of PTM: increased application accuracy and decreased input volume (Warneke et al., 2021).

The experiences of turfgrass managers who have adopted this technology have been primarily positive, with users reporting improved accuracy in applications and a reduction in total areas treated (Floyd et al., 2024; Richman, 2019). When compared to manual sprayer applications, the implementation of GNSS technology has been shown to reduce spraying errors, such as non-target, missed, or overlapping applications, resulting in up to a 4.6% reduction in total volume applied to athletic fields (Floyd et al., 2024). A study by Booth et al. (2021) found that targeted fungicide applications reduced fungicide inputs by up to 65% while controlling spring dead spot (*Ophiosphaerella* spp.) outbreaks. However, the authors note that further research is necessary to refine methods for site-specific applications, including optimizing the size of targets sprayed. In another study using a GNSS-guided sprayer for targeted spring dead spot fungicide applications, Henderson et al. (2025) reduced inputs by 48% on average while maintaining control of the disease similar to full-coverage applications.

Despite their potential benefits, targeted pesticide applications using GNSS-guided sprayers remain limited in the turfgrass industry. A survey of golf course superintendents revealed that while general knowledge of variability within turfgrass areas exists, precise data quantifying the advantages of site-specific management is still necessary (Straw et al., 2020). Several barriers contribute to this limited adoption, including the high initial cost of equipment, difficulties in training staff, and concern about the technology's efficacy (Price et al., 2023). In particular, limited quantitative

evidence on the accuracy and precision of targeted pesticide applications deters widespread acceptance. Risk aversion among potential adopters is heightened by the limited track record of GNSS-guided sprayers in commercial agriculture, indicating that the technology must be widely demonstrated to encourage adoption (Warneke et al., 2021). To support this process, the establishment of proven, standardized protocols is essential for enhancing the perceived reliability of the technology and promoting the broader acceptance and effective use of site-specific PTM strategies (Bell et al., 2013). To promote the adoption of PTM practices in the turfgrass industry, further quantifiable research is essential (Braun et al., 2023).

There is a clear need for research that evaluates the performance of targeted pesticide applications made with GNSS-guided sprayers. Key metrics such as accuracy and precision are critical to understanding the effectiveness of these systems. Additionally, real-world factors, such as sprayer travel speed and target coverage size, may significantly influence the effectiveness of targeted applications but remain insufficiently characterized in current literature. This study seeks to address these gaps by quantitatively assessing the accuracy and precision of GNSS-equipped sprayers in targeted pesticide applications under varying operational parameters of target size and sprayer travel speed. Quantifying the variability in the accuracy and precision of targeted applications using a GNSS-equipped sprayer at different traveling speeds will provide turfgrass managers with information to make a more informed decision on whether to adopt this precision management strategy. It is hypothesized that sprayer travel speed and target size will significantly affect the accuracy and precision of targeted pesticide

applications using GNSS-guided sprayers, with reduced accuracy and precision anticipated at higher travel speeds and smaller target sizes.

Materials and Methods

The trial was conducted at the Virginia Tech Golf Course and tested three different travel speeds, 4.8, 7.2, and 9.7 km/h, and three target sizes 0.5, 1, and 2 meters in diameter. Target centers were marked and mapped using a real-time kinematic (RTK) GNSS receiver and were integrated into the Toro GeoLink (The Toro Company, Bloomington, MN, USA) system for precise nozzle control. A fluorescent dye solution (Bright Dyes, Jackson, MS, USA) was applied using a Toro MultiPro 5800 sprayer, and each trial was repeated three times. Following application, UV imaging with a drone captured deposition patterns, which were analyzed in Fiji/ImageJ (Schindelin et al., 2012) to calculate offset distance, overlap percentage, and overspray area, providing detailed metrics on application accuracy across treatments.

Study Site and Experimental Design

The study was conducted on a mixed-species fairway, primarily composed of perennial ryegrass (*Lolium perenne* L.) and Kentucky blue grass (*Poa pratensis* L.), at the Virginia Tech Golf Course in Blacksburg, Virginia (37.2279, -80.4337) between October and December 2024. A 29 m x 144 m section of the fairway was selected for the trial area due to its uniform turfgrass and minimal topographic variation. Before trial initiation, the fairway was mown to a standard golf course fairway height of 1.9 cm. The three sprayer travel speeds were chosen to capture the range of travel speeds commonly used in

pesticide spray applications (Cornell University Cooperative Extension, 2021; The Toro Company, 2018). The three target sizes were used to represent real-world variation in the sizes of spot-treatment areas and buffer sizes adopted from methods and suggestions by Booth et al. (2021) and Henderson et al. (2025).

The trial area was divided into three rectangular strips, measuring 5.5 m by 144 m with 3 m buffers between each section. Each strip was randomly assigned one of the tested sprayer travel speeds. The trial area was split in this manner to facilitate operating the sprayer at a single constant speed using the ground-speed-lock function across the entire length of each section, ensuring consistency of speed and forming a reliable basis for comparison among speeds. Within each strip, three target sizes, 0.5 meters, 1 meter, and 2 meters in diameter, were randomly placed, with 12 replicated targets per size. This resulted in a total of 36 targets per strip and an overall total of 108 targets per trial run. The random placement ensured that each target size was distributed without bias within each speed block. The trial was repeated three times, with the trial repetition serving as the blocking factor of the experiment. This experimental design meets the requirements of a split plot randomized complete block design, with travel speed as the main plot factor, target size as the sub plot factor, and trial repetition as the blocking factor.

To facilitate data collection, 5.5 m by 3.7 m blocks were marked along each of the three trial strips. These blocks were used to standardize the positioning of the portable ultraviolet (UV) lighting rig and capture drone imagery under uniform illumination. Once imaging was completed in one section, the lighting rigs were moved sequentially through all sections until every target in the larger study area had been documented, following procedures described by Koo et al. (2025).

Marking and Mapping Target Centers

Once the trial area was measured and delineated, the 12 targets per size were randomly placed within each strip, with each target's center marked and mapped. An 8 cm dot was marked at the center of each target using fluorescent orange paint (Rust-Oleum, Vernon Hills, IL, USA) for visibility in the drone imagery described below. The precise location of the target centers was mapped using an Emlid rs+ (Emlid, Budapest, Hungary) GNSS receiver configured as a rover. The Emlid rs+ rover was connected to the same Topcon (Topcon, Tokyo, Japan) Networked Transport of RTCM via Internet Protocol (NTRIP) caster utilized by the Toro sprayer's GeoLink system. The rover was set to receive corrections from Topcon NTRIP through a mobile phone acting as a bridge, providing spatial measurements accurate to within 2 cm. The Emlid Flow application (Emlid, Budapest, Hungary) was used to log each target's center coordinates, which were stored as RTK data containing longitude, latitude, ellipsoidal height, and associated root mean square (RMS) error parameters.

After mapping all target centers, the data were exported as a comma-separated values (.csv) file. This file was imported into ArcGIS Pro (ArcGIS Desktop v10.5.1, Environmental Systems Research Institute, Redlands, CA) and displayed as XY Data with longitude set as X, latitude as Y, and the coordinate system defined as World Geodetic System 1984 (WGS 84) to maintain consistency with the Toro GeoLink's operating coordinates. Each target center was then overlaid with a buffer measuring 0.5 m, 1.0 m, or 2.0 m in diameter, generating circular polygons representing the intended treatment zones. Next, the buffer layers were dissolved with their associated target center

points, creating a single shapefile for each target that included both center coordinates and the circular boundary. This final shapefile (Figure 1) was uploaded to the GeoLink system on the Toro sprayer, allowing the operator to create a spray job that triggered nozzles precisely over each buffered target.



Figure 1: ArcGIS Pro shapefile map depicting targets randomly placed throughout each travel speed strip.

Sprayer Setup and Application Procedure

A Toro MultiPro 5800 (The Toro Company, Bloomington, MN) sprayer equipped with Real-Time Kinematic (RTK) GNSS guidance through the GeoLink Precision Spray System and multi-section nozzle control was used to ensure precise activation or deactivation of individual nozzles when crossing defined buffer zones. The RTK corrections allow for sub-2 cm positional accuracy, which allows for the detection of fine-scale differences in spray deposition at varying speeds. Before trial initiation, the sprayer was calibrated by measuring flow rates from each nozzle at the set standard operating pressure of 276 kPa, verifying uniform output across the boom. The sprayer

was equipped with 12 nozzle mounts, each fitted with TeeJet AI11008-VS Flat Tip nozzles (TeeJet® AI11008-VS, Spraying Systems, Wheaton, IL).

A biodegradable, fluorescent xanthene dye (Bright Dyes, Jackson, MS, USA) was mixed into the tank solution at a rate of 40 ml dye L⁻¹. The dye-to-water ratio was determined to be the optimal rate by a pilot study, which found that 1 ml of dye per 25 ml of water provided the most visibility-intense fluorescent glow without over-saturating the turfgrass canopy.

To apply the dye, the sprayer drove at a consistent speed, making one straight pass over each of the three sections. The predetermined sprayer travel speed was randomly assigned to each section, and the speed was maintained using the built-in ground-speed-lock switch. The sprayer was brought to speed and locked outside the test site and prior to passing over the first subsample. During each pass, the GeoLink software automatically engaged or disengaged the nozzles as the sprayer moved into or out of each target zone. Ambient conditions, including wind speed, temperature, and relative humidity, were measured using a handheld instrument to document any environmental factors affecting droplet movement or evaporation. Spraying was not conducted if wind speeds exceeded 16 km/h based on local guidelines for safe pesticide applications (VGCSAA, 2020).

UV Imaging and Data Collection

Immediately following each application, the study area was illuminated by a portable structure mounted with six 50-W 365 nanometer (nm) ultraviolet (UV) lights (Everbeam, British Columbia, Canada) in accordance with procedures described by Koo

et al., 2024). The lights were evenly spaced 1.8 m apart along the edges of each plot to achieve uniform illumination and minimize shadow effects. A DJI Mavic 2 Advanced Enterprise drone equipped with a 48MP, ½” CMOS, RGB sensor (DJI, Shenzhen, China), flown at a fixed altitude of 5 m above ground, captured high-resolution images of each plot. Camera settings (ISO, shutter speed, and white balance) were standardized to factory settings to maintain consistency among images. TIFF file formats were used to ensure maximum data retention for subsequent analysis.

In this study, accuracy of the sprayer refers to the proximity of the actual sprayer deposition to the intended target, measured by the distance between the center of the sprayer deposition and target centroid, and by the percentage of overlapping area between the sprayed area and intended target area. Precision refers to the consistency of applications across repeated trials, evaluated by analyzing the variability in offset distances and uniformity of spray deposition around target centers for each treatment.

Data and Statistical Analysis

All images were analyzed in Fiji, an enhanced distribution of the imaging software ImageJ (Schindelin et al., 2012) to measure both the accuracy and precision of the sprayer’s deposition relative to the intended target centers. To calibrate the scale in each image and ensure the consistency of data collected, each plot was demarcated with fluorescent orange paint at each corner, providing a known dimension of 5.5 m x 3.7 m. In Fiji, the Straight Line Tool was used to draw a line across the known 5.5-meter distance. Using the "Analyze > Set Scale" function, the pixel length of this line was calibrated by entering the known real-world distance (5.5 m). The scale was then verified

by measuring the known 3.7 m sides of the plot to confirm accuracy. The scale was then set for that image, ensuring all subsequent measurements in the image were reported in real-world units.

Once the scale was defined, circles representing each intended target size were overlaid and centered on the intended target center, indicated by the orange-painted dots. Then, the actual dye deposition was outlined by freehand selection, marking the area in which the sprayer deposited the dye. The software's Analyze > Measure tool returned the area and centroid coordinates (X, Y) of each dye-marked spot. Drawing a straight line between the intended target center (indicated by fluorescent orange paint) and the dyed centroid returned an offset distance, or the distance between the intended target and actual sprayer deposition, reflecting the accuracy of the sprayer's application. The area of overlap between the intended target and actual sprayer deposition was computed by measuring the area of their intersection. Dividing this intersection by the area of the intended target produced a percentage coverage measure. Any directional tendencies in offset were determined by subtracting the intended target's center coordinates from those of the actual deposit centroid. The resulting coordinate differences were then translated into standard compass directions (e.g., North, Northeast, East) using Cartesian grid logic, where positive or negative differences along the X and Y axes corresponded to specific directional categories. Overspray was calculated by subtracting the area of the intended target from the area of the actual spray deposition to measure the area of dye applied outside the intended target area.

The collected data were subject to analysis of variance (ANOVA) testing, utilizing a significance level of 0.05 followed by Tukey's HSD test to identify group

differences in JMP Pro 18 (SAS Institute Inc., Cary, NC, USA). Separate least-squares means models were fitted for each response variable of offset distance, area of overlap, percent coverage, and overspray. Residual diagnostics performed using the Shapiro-Wilk test for normality and Levene's test for homogeneity of variance confirmed that assumptions for parametric analysis were satisfied or appropriately addressed.

Results

The results of the analysis indicated that trial run had no significant effect on any of the measured responses (Table 1). Therefore, data were analyzed collectively across all three runs to determine the effects of sprayer speed (4.8, 7.2, 9.7 km/h), target size (0.5, 1, 2 m), and their interaction.

Table 1: Analysis of variance (ANOVA) results evaluating the significance ($P < 0.05$) of the main effects of travel speed, target size, trial run, and their interactions on % overlap, offset distance, and overspray area. Significant effects are indicated in bold.

	% Overlap	Offset Distance (m)	Overspray Area (m²)
Speed	<.0001	<.0001	<.0001
Target Size	0.0949	0.2542	<.0001
Trial Run	0.6581	0.1169	0.9718
Speed*Size	0.2034	0.2031	<.0001
Speed*Run	0.2855	0.1273	0.9935
Size*Run	0.8847	0.4976	0.2168
Speed*Size*Run	0.7370	0.5550	0.1096

Sprayer speed significantly influenced percent overlap, offset distance, and overspray area (Table 1). Spraying at the slowest speed, 4.8 km/h, resulted in significantly lower overlap of the intended target (60.3%) compared to the higher speeds of 7.2 km/h (98.4%) and 9.7 km/h (96.5%), which were not significantly different from each other (Table 2). Offset distances followed a similar pattern; the average offset at 4.8 km/h (0.87 m) was significantly larger than the offsets at both 7.2 km/h (0.31 m) and 9.7 km/h (0.43 m), while no significant difference was observed between the two faster speeds (Table 2).

Table 2. Main effect of sprayer operational speed on percentage overlap and offset distance of precision spray averaged over three target sizes and three trials. Means not connected by the same letter are significantly different at $P < 0.05$.

Speed (km/h)	% Overlap	Offset Distance (m)
4.8 km/h	60.299 (B)	0.86628 (A)
7.2 km/h	98.396 (A)	0.30879 (B)
9.7 km/h	96.510 (A)	0.43042 (B)

Overspray area showed a significant main effect of both speed and target size, as well as an interaction between these two factors (Table 3). In general, higher speeds and larger target diameters substantially increased overspray area. The increase in overspray area is more pronounced at larger target sizes as speed increased, with minimal overspray (0.57 m²) recorded when spraying 0.5 m targets at 4.8 km/h, whereas maximum overspray (4.16 m²) occurred with the 2 m targets at the highest travel speed (9.7 km/h).

This indicates that overspray not only increases with travel speed and target size individually, but that the interaction of the two factors amplifies the effect at larger target sizes, demonstrated by the difference in the effect of speed becoming more pronounced as target size increases.

Table 3. Interaction of speed by target size on overspray area of precision spray averaged over three trials. Means not connected by the same letter are significantly different at $P < 0.05$.

Speed (km/h)	0.5 m Target	1 m Target	2 m Target
4.8 km/h	0.5665 (B)	0.8330 (B)	1.6437 (C)
7.2 km/h	0.8958 (A)	1.8393 (A)	3.5097 (B)
9.7 km/h	1.1593 (A)	2.1233 (A)	4.1597 (A)

Despite significant speed effects on offset distance, percent overlap, and overspray, nominal logistic analysis revealed that offset direction was unaffected by sprayer speed, target size, or trial run ($p > 0.05$). Nevertheless, there was a strong and consistent directional bias: approximately 90% of offsets were located south, southeast, or southwest of the intended targets, though the distance of offset varied. This directional bias and the dispersion of actual spray centroids for each speed and target size combination is illustrated in Figure 2.

Precision Visualization: Actual Spray Centroids by Target Size and Speed

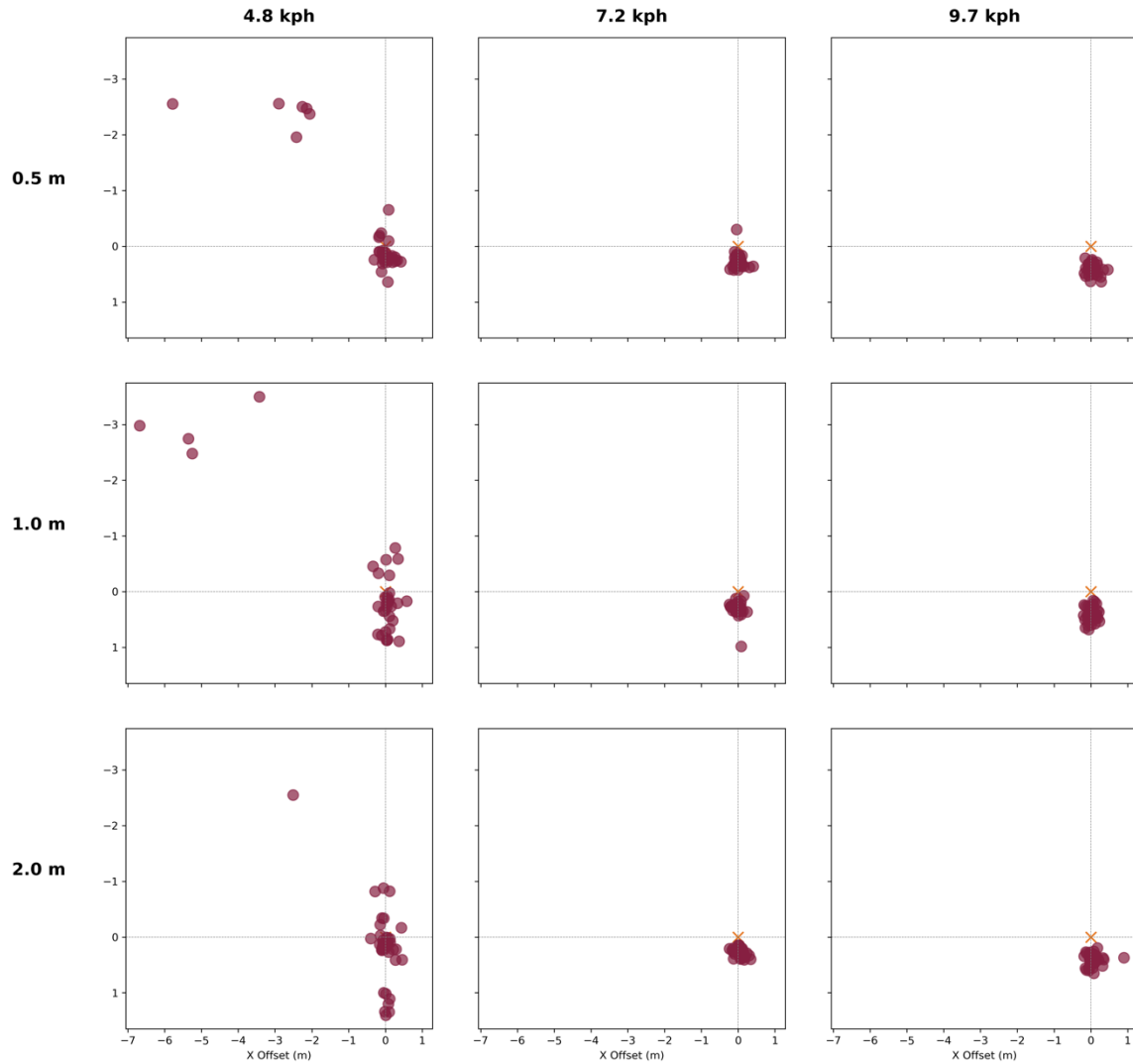


Figure 2: The distribution of spray centroids relative to the intended target center, represented by an orange X, with maroon dots indicating actual spray centroid locations.

Discussion

The results of this study provide quantitative evidence that GPS-guided, site-specific spraying can achieve a high degree of accuracy and precision in turfgrass

management. The majority of targeted spray applications were confined to the intended treatment areas, indicating that the sprayer's RTK-based guidance and individual nozzle control effectively minimized off-target application, aligning with prior research demonstrating precision sprayer's ability to treat designated spots with minimal deviation (Villette et al., 2021). The intermediate and higher speeds of 7.2 and 9.7 km/h demonstrated significantly greater overlap percentages and smaller offset distances compared to the lower speed of 4.8 km/h, which showed lower overlap and a larger offset distance. These results are consistent with research by Sharda et al. (2013), who found that targeted applications made while traveling 6.4 km/h or slower had a significantly higher rate of errors, likely due to delays in nozzle actuation or extended response times when transitioning into and out of target zones.

Target size alone had no significant impact on the offset distance and percent overlap, indicating the sprayer maintained consistent positional accuracy and precision of applications across varying target dimensions. Consistent accuracy and precision of applications across target sizes indicates that turfgrass managers can implement spot-treatment strategies for a range of applications, from small-scale weed infestations to large areas affected by disease. However, these findings are specific to the specific sprayer used for this study. Simulation studies have cautioned that targeted application efficacy is influenced by nozzle spacing on the sprayer boom, with narrow spacing (0.5 m) greatly improving the accuracy of small target applications (Villette et al., 2021). The consistent performance across target sizes also supports findings by Rasmussen et al. (2020), who found the limiting factors in targeted applications to be primarily

technological, relating to the boom section width and sprayer control system responsiveness, rather than the size of the intended target.

A significant interaction between sprayer speed and target size was observed for overspray area. Higher travel speeds and larger targets resulted in increased overspray, which reflects the known challenge of nozzle actuation lag at higher speeds documented by Rasmussen et al. (2020). Despite incidental overspray, the overall area treated was 81.04% less than if a full-coverage broadcast application had been applied to the entire trial area. This supports prior research by Booth et al. (2021) and Henderson et al. (2025), who found targeted applications significantly decreased the amount of product applied and the overall area sprayed.

These results directly address concerns regarding the efficacy and accuracy of GNSS-guided sprayer technologies, potentially mitigating some barriers hindering broader industry adoption. Historically, adoption of PTM technologies in turfgrass management has been limited by uncertainty regarding performance and operational constraints (Price et al., 2023). Demonstrating reliable accuracy across operational conditions may increase turf managers' confidence in adopting targeted application methods, providing empirical support to encourage implementation.

Future research should replicate and extend these findings using diverse sprayer models and GNSS systems under different geographic locations, environmental conditions, and operational scenarios. A study by Franco et al. (2017) found that pesticide savings when making targeted applications depend not only on the sprayer's spatial precision, but also on the target spatial distribution, finding that many scattered targets were more challenging to hit than few, large clusters. These findings highlight the need

for continued research into the efficacy of targeted applications made across diverse turfgrass conditions and pest distributions. Studies investigating interactions between weather conditions (e.g., wind, humidity) and sprayer accuracy are warranted. Additional trials involving various pesticides, including fungicides, herbicides, and insecticides, would further validate accuracy and precision across chemical formulations and nozzle types. Research investigating long-term implementation of GNSS-guided applications across multiple seasons and diverse turfgrass systems would provide insights into cumulative economic benefits, chemical reduction, and pest management efficacy.

In conclusion, this study provides quantitative insights into operational factors influencing GNSS-guided pesticide applications in turfgrass systems. The outcomes suggest that GNSS-guided sprayers can apply pesticides at operationally relevant speeds and varying target sizes, supporting PTM objectives of reducing chemical inputs while maintaining accurate and precise spray delivery to targeted pests. Additional research addressing calibration requirements and broader operational conditions is essential for facilitating wider adoption of GNSS-guided spraying technologies in turfgrass management.

Bibliography

1. Beard, J. B., & Green, R. L. (1994). The Role of Turfgrasses in Environmental Protection and Their Benefits to Humans. *Journal of Environmental Quality*, 23(3), 452–460. <https://doi.org/10.2134/jeq1994.00472425002300030007x>
2. Bell, G. E., Kruse, J. K., & Krum, J. M. (2013). The Evolution of Spectral Sensing and Advances in Precision Turfgrass Management. In *Turfgrass: Biology, Use, and Management* (pp. 1151–1188). <https://doi.org/10.2134/agronmonogr56.c30>
3. Booth, J. C., Sullivan, D., Askew, S. A., Kochersberger, K., & McCall, D. S. (2021). Investigating Targeted Spring Dead Spot Management via Aerial Mapping and Precision-Guided Fungicide Applications. *Crop Science*, 61(5), 3134–3144. <https://doi.org/10.1002/csc2.20623>
4. Braun, R. C., Mandal, P., Nwachukwu, E., & Stanton, A. (2024). The Role of Turfgrasses in Environmental Protection and Their Benefits to Humans: Thirty Years Later. *Crop Science*, 64(6), 2909–2944. <https://doi.org/10.1002/csc2.21383>
5. Braun, R. C., Straw, C. M., Soldat, D. J., Bekken, M. A. H., Patton, A. J., Lonsdorf, E. V., & Horgan, B. P. (2023). Strategies for Reducing Inputs and Emissions in Turfgrass Systems. *Crop, Forage & Turfgrass Management*, 9(1), e20218. <https://doi.org/10.1002/cft2.20218>
6. Carlson, M. G., Gaussoin, R. E., & Puntel, L. A. (2022). A Review of Precision Management for Golf Course Turfgrass. *Crop, Forage & Turfgrass Management*, 8(2), e20183. <https://doi.org/10.1002/cft2.20183>
7. Carrow, R. N., Krum, J. M., Flitcroft, I., & Cline, V. (2010). Precision Turfgrass Management: Challenges and Field Applications for Mapping Turfgrass Soil and Stress. *Precision Agriculture*, 11(2), 115–134. <https://doi.org/10.1007/s11119-009-9136-y>
8. Cornell University Cooperative Extension. (2021). Sprayer Calibration. <https://core.psep.cce.cornell.edu/Tutorials/core-tutorial/module19/index.aspx>
9. Floyd, W. W., Muesse, M. R., Tucker, H. N., Alabi, O. E., Winger, J. O., & Straw, C. M. (2024). Assessing Application Errors on Sports Fields Across Varying Levels of Sprayer Technology and Operator Experience. *Crop, Forage & Turfgrass Management*, 10(2), e20301. <https://doi.org/10.1002/cft2.20301>
10. Franco, C., Pedersen, S. M., Papaharalampos, H., & Ørum, J. E. (2017). The Value of Precision for Image-Based Decision Support in Weed Management. *Precision Agriculture*, 18, 366–382. <https://doi.org/10.1007/s11119-017-9520-y>
11. Gels, J. A., Held, D. W., & Potter, D. A. (2002). Hazards of Insecticides to the Bumble Bees *Bombus impatiens* (Hymenoptera: Apidae) Foraging on Flowering White Clover in Turf. *Journal of Economic Entomology*, 95(4), 722–728. <https://doi.org/10.1603/0022-0493-95.4.722>

12. Haith, D. A. (2010). Ecological Risk Assessment of Pesticide Runoff from Grass Surfaces. *Environmental Science & Technology*, 44(16), 6496–6502. <https://doi.org/10.1021/es101636y>
13. Henderson, C., Haak, D., Mehl, H., Shafian, S., & McCall, D. (2025). Precision Mapping and Treatment of Spring Dead Spot in Bermudagrass Using Unmanned Aerial Vehicles and Global Navigation Satellite Systems Sprayer Technology. *Precision Agriculture*, 26(2), 38. <https://doi.org/10.1007/s11119-025-10231-7>
14. Koo, D., Godara, N., Cubas, J. R. R., & Askew, S. D. (2025). A Method to Spatially Assess Multipass Spray Deposition Patterns via UV Fluorescence and Weed Population Shifts. *Crop Science*, 65(1), e21377. <https://doi.org/10.1002/csc2.21377>
15. Krum, J. M., Carrow, R. N., & Karnok, K. (2010). Spatial Mapping of Complex Turfgrass Sites: Site-Specific Management Units and Protocols. *Crop Science*, 50(1), 301–315. <https://doi.org/10.2135/cropsci2009.04.0173>
16. Luck, J. D., Pitla, S. K., Shearer, S. A., Mueller, T. G., Dillon, C. R., Fulton, J. P., & Higgins, S. F. (2010). Potential for Pesticide and Nutrient Savings via Map-Based Automatic Boom Section Control of Spray Nozzles. *Computers and Electronics in Agriculture*, 70(1), 19–26. <https://doi.org/10.1016/j.compag.2009.08.003>
17. Price, K., Kitchin, E. C. A., Kumari, S., McCall, D. S., & Posadas, B. (2023). Understanding Human Perceptions Limiting the Adoption of Precision Turfgrass Management. ASA, CSSA, SSSA International Annual Meeting.
18. Rasmussen, J., Azim, S., Nielsen, J., Mikkelsen, B., Hørfarter, R., & Christensen, S. (2020). A New Method to Estimate the Spatial Correlation Between Planned and Actual Patch Spraying of Herbicides. *Precision Agriculture*, 21, 713–728. <https://doi.org/10.1007/s11119-019-09691-5>
19. Richman, H. (2019, November). GPS Technology in Golf Course Management. *Golf Course Magazine Online*. <https://www.gcmonline.com/tags/gps-golf-course-management>
20. Schindelin, J., Arganda-Carreras, I., Frise, E., Kaynig, V., Longair, M., Pietzsch, T., Preibisch, S., Rueden, C., Saalfeld, S., & Schmid, B. (2012). Fiji: An Open-Source Platform for Biological-Image Analysis. *Nature Methods*, 9(7), 676–682. <https://doi.org/10.1038/nmeth.2019>
21. Sharda, A., Luck, J. D., Fulton, J. P., McDonald, T. P., & Shearer, S. A. (2013). Field Application Uniformity and Accuracy of Two Rate Control Systems with Automatic Section Capabilities on Agricultural Sprayers. *Precision Agriculture*, 14, 307–322. <https://doi.org/10.1007/s11119-012-9296-z>
22. Straw, C. M., Wardrop, W. S., & Horgan, B. P. (2020). Golf Course Superintendents' Knowledge of Variability Within Fairways: A Tool for

- Precision Turfgrass Management. *Precision Agriculture*, 21(3), 637–654. <https://doi.org/10.1007/s11119-019-09687-1>
23. The Toro Company. (2018). Multi Pro 5800 User Manual. <https://manuals.toro.com/168250/index.html>
24. Villette, S., Maillot, T., Guillemin, J.-P., & Douzals, J. (2021). Simulation-aided Study of Herbicide Patch Spraying: Influence of Spraying Features and Weed Spatial Distributions. *Computers and Electronics in Agriculture*, 182, 105981. <https://doi.org/10.1016/j.compag.2020.105981>
25. Virginia Golf Course Superintendents Association of America (VGCSAA). (2020). Environmental Best Management Practices for Virginia’s Golf Courses, 2nd Edition. https://www.gcsaa.org/docs/default-source/environment/virginia-bmps-second-edition.pdf?sfvrsn=8639f03e_2
26. Warneke, B. W., Zhu, H., Pscheidt, J. W., & Nackley, L. L. (2021). Canopy Spray Application Technology in Specialty Crops: A Slowly Evolving Landscape. *Pest Management Science*, 77(5), 2157–2164. <https://doi.org/10.1002/ps.6167>

Chapter 3: Leveraging Deep Learning for Dollar Spot Detection and Quantification in Turfgrass

Abstract:

This study evaluates the effectiveness of fine-tuning a semantic segmentation model to identify and quantify dollar spot in turfgrasses, the most extensively managed and researched disease of turfgrasses worldwide. Using the DeepLabV3+ model, recognized for its capability to segment complex shapes and integrate multi-scale contextual information, the research leveraged a diverse dataset comprising various turfgrass species, disease stages, and lighting conditions to ensure robust model training. The trained model can identify and segment disease instances accurately and precisely, and the results indicate the potential for model-based assessment to outperform traditional visual assessment methods in speed, accuracy, and consistency, pending direct comparison. By fine-tuning a pretrained semantic segmentation model, we adapted it for disease segmentation using only a standard personal computer's graphics processing unit. This approach highlights the practicality of deploying advanced deep learning applications in turfgrass pathology with limited computational capacity. The proposed model provides a new tool for turfgrass researchers and professionals to rapidly and accurately quantify this important disease under real-world growing conditions. Additionally, the findings suggest the potential to apply deep learning algorithms to other turfgrass diseases to support data-driven decisions. This could enhance disease management practices and improve decision-making processes for fungicidal treatments, thereby improving the economic and environmental sustainability of turfgrass management.

Introduction

The benefits of turfgrass are intertwined with modern society due to its wide range of environmental, recreational, and aesthetic applications (Stier et al., 2015). Turfgrass supports erosion control (Krenitsky et al., 1998), groundwater filtration (Monteiro, 2017), and urban heat dissipation (Peters et al., 2011). It serves as a safe, affordable surface for sports with aesthetic benefits to surrounding landscapes (Beard & Green, 1994). Across various roles and landscapes, consumers prefer turfgrasses with high aesthetic quality (Barnes et al., 2020; Jung & Chung, 2024; Yue et al., 2021).

High expectations in turfgrass appearance and playability require diligent management, including the control of turfgrass diseases (Vargas, 2018). One such disease is dollar spot, caused by several *Clariireedia* spp., which affects all cultivated warm- and cool-season turfgrass species, including annual bluegrass (*Poa annua* L.), creeping bentgrass (*Agrostis stolonifera* L.), bermudagrass (*Cynodon dactylon* L.), and zoysiagrass (*Zoysia japonica* Steudel) (Goodman & Burpee, 1991). Its symptoms include the development of lesions on affected leaves that progress from chlorotic to water-soaked and finally bleached (Tredway et al., 2022). Patches may appear white or straw-colored (Walsh et al., 1999), with sunken spots ranging in size from 7 to 15 cm, appearing as the disease progresses (Sapkota et al., 2022). Under certain conditions, a cottony or spider web-like growth of mycelium may appear on affected turf (Tredway et al., 2022). It can be costly to manage, making dollar spot one of the most economically significant turfgrass diseases (Salgado-Salazar et al., 2018).

Effective management strategies hinge not only on understanding its manifestations but also on the precise assessment of its severity. Disease quantification is critical to

creating disease forecasts, decision thresholds, and accurate analyses of treatment effects, and it directly influences the decision to apply or withhold fungicidal treatment (Bock et al., 2020). Despite this, most assessments are performed manually and require a trained pathologist or turfgrass professional to scout for and identify diseases in crops (Shahi et al., 2023). Traditional methods for assessing disease severity have relied on visual estimation, a technique disposed to subjectivity and significant variation among raters (Bock et al., 2020; Nutter et al., 1993; Schwanck & Del Ponte, 2014). This method not only requires the expertise of trained professionals but is also notably time-consuming (Thomas et al., 2018). The subjectivity of visual assessments, along with their need for specialized skills and time, motivates the exploration of a more objective and efficient approach.

One method that seeks to solve this subjectivity and provide accurate disease analysis is digital image analysis (DIA). Richardson et al. (2001) described DIA as capturing digital images of turfgrass and analyzing the images to quantify various parameters, including turfgrass cover and color. The process includes acquiring high-quality images with consistent lighting conditions, selecting appropriate portions of the image, and quantifying the desired parameters using specialized software. Although the acquisition of proper images can be challenging, this method significantly reduces evaluator bias and enhances data precision and consistency compared to traditional visual assessments. There has been success with using DIA to evaluate diseases on turfgrass, including assessing brown patch (*Rhizoctonia solani*) (Sykes et al., 2020), spring dead spot (*Ophiosphaerella* spp.) (Tomaso-Peterson, 2008), and dollar spot (Horvath & Vargas, 2005). However, a notable limitation of DIA is its difficulty delineating one

specific disease when other stresses are present on the turf, including other diseases, drought, mower scalping, and fertility issues (Karcher & Richardson, 2013). This limitation can create issues when using DIA for the identification and quantification of a single disease on turfgrass. Given this constraint, a solution that can provide rapid, accurate, and consistent disease quantification in complex scenarios is still necessary.

The constantly advancing field of computer science provides new opportunities to rapidly and nondestructively quantify turfgrass diseases and other pests. Deep learning, an advanced subset of machine learning characterized by its use of deep neural networks for hierarchical feature extraction and analysis, has proven effective for segmenting plant diseases (Miao et al., 2020). Deep learning models can provide accurate and efficient solutions for detecting disease in plants (Liu & Wang, 2021), offering a compelling alternative to traditional manual disease identification and quantification methods.

While there has been limited application of deep learning with turfgrass diseases specifically, studies have shown machine learning's efficacy in creeping bentgrass (*Agrostis stolonifera*) yield predictions (Zhou & Soldat, 2021) and in turfgrass weed detection (Yu et al., 2019). In other crops, deep learning models have been successful in identifying diseases in cereal grains (Waldamichael et al., 2022), tomatoes (Durmus et al., 2017), and soybeans (Yu et al., 2022).

With regard to plant disease detection, deep learning works in three distinct steps: classification, detection, and segmentation (Wang, 2016). Classification involves identifying the presence or absence of a disease through feature expression and determining if the features match those of the intended disease. Detection is centered around locating where the disease is present in the image. Finally, segmentation

delineates the exact shape and extent of the disease by outlining the affected areas at the pixel level. This separates the lesions or damage from the healthy parts of the plant, providing details on the size, shape, and severity of the disease (Boulent et al., 2019).

Semantic segmentation models, a specialized type of deep learning model designed for pixel-wise classification, classify each pixel of an image into a category predefined by its developers. This facilitates precise mapping of disease spread within plant imagery, enabling detailed and accurate assessment of the affected areas (Garcia-Garcia et al., 2017). This pixel-wise classification is critical for applications where the exact delineation of diseased versus healthy tissue informs treatment and management decisions.

Deep learning surpasses traditional machine learning and manual methods in disease identification and quantification by automating feature extraction, ensuring consistency, and enhancing scalability (Hasan et al., 2020). Deep learning semantic segmentation models are able to overcome technical limitations in disease identification (Boulent et al., 2019) and learn features of the target disease with limited manual interference (Liu & Wang, 2021). These advantages and the specialized capabilities of deep learning models in enhancing disease identification with minimal manual intervention motivated the decision to use semantic segmentation to identify and quantify dollar spot disease in turfgrass.

By automating the dollar spot assessment process, we seek to provide an alternative method to rapidly and accurately assess dollar spot incidence for both the scientific and turfgrass professional communities. In doing so, we hope to provide scientists with an objective tool to accurately and rapidly quantify dollar spot development for expedited

data collection and turfgrass professionals with a new decision-support tool to guide the need for fungicide applications.

Materials and Methods

2.1 Model selection

The objective of the model is to enable accurate quantification of dollar spot disease given an image of affected turfgrass. In the field of computer vision, there are several fundamental tasks that enable machines to interpret and understand visual data. Among these tasks are image classification, object detection, and semantic segmentation (Feng et al., 2019). Image classification assigns a label or category to an entire image to identify its primary subject. While determining that dollar spot disease is present in an image is necessary for this project, identification alone is not sufficient for quantification.

Similarly, object detection involves identifying and locating objects within an image, often using bounding boxes or more precise methods to specify their positions. Although an object detection model could be trained to identify occurrences of dollar spot in turfgrass, it may not provide the fine granularity needed to accurately quantify the severity of the disease, which is characterized by irregular patches and lesions.

Alternatively, semantic segmentation classifies each pixel in an image. This pixel-level precision makes it highly effective at delineating the edges of each disease instance (Figure 1).

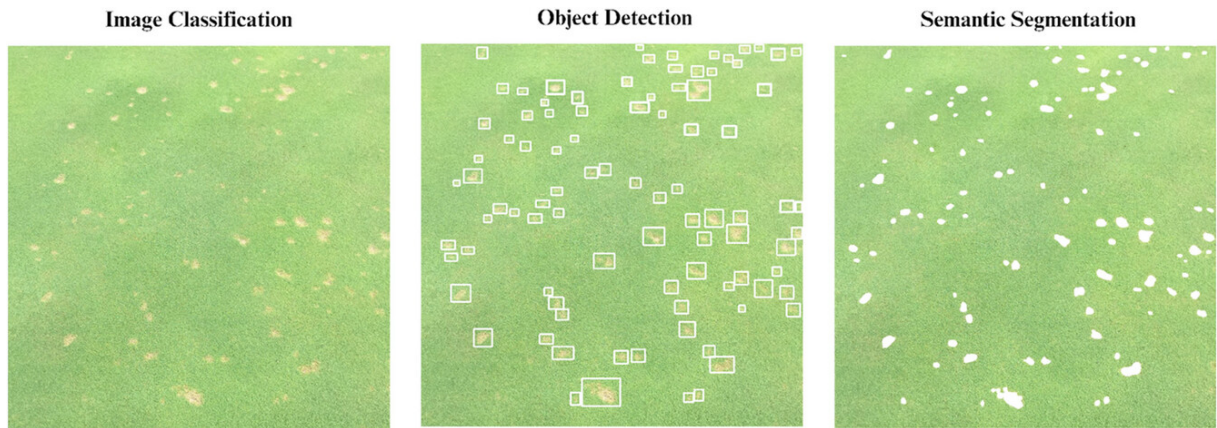


Figure 1: A visualization of computer vision tasks categorizing dollar spot on turfgrass. For the image classification task, the image is classified as containing dollar spot since it is the prevailing disease afflicting the turfgrass. For the object detection task, bounding boxes are drawn around each instance of dollar spot. For the semantic segmentation task, the model predicts the binary probability that each pixel represents dollar spot, creating masks that identify affected areas.

The DeepLabV3+ machine learning model, developed by Google (Alphabet, Inc.), was adopted for this study using methods described by Chen et al. (2018). This model was chosen due to its proficiency in segmenting irregular shapes, which are characteristic of dollar spot infections. The model achieves this performance through the integration of atrous spatial pyramid pooling with an encoder-decoder architecture, employs atrous convolution to control feature map resolution effectively, and captures contextual information at multiple scales with reduced computational costs (Chen et al., 2018). These features enable DeepLabV3+ to effectively combine detailed spatial information with broad contextual understanding, making it adept at segmenting objects with irregular contours like those of our target class. DeepLabV3+ also demonstrates superior

performance on benchmarks like PASCAL VOC 2012 and Cityscapes without post-processing (Chen et al., 2018). Though it has yet to be used with turfgrass, DeepLabV3+ has shown success when used for the segmentation of rice leaf diseases (Li et al., 2023) and corn leaf diseases (Divyanth et al., 2023).

2.2 Image dataset and augmentation

The majority of this project's dataset consists of field research images from dollar spot trials conducted by the turfgrass pathology research programs at Virginia Tech and North Carolina State University. These images contain turfgrass in which either natural infestations of dollar spot have occurred or asymptomatic grass has been inoculated with the dollar spot pathogen. All instances of dollar spot in images were confirmed by trained turfgrass pathologists at Virginia Tech. These images were not pruned for purity, and no foreign objects, such as wooden stakes, water meters, or leaves, were removed if they were present. The model benefits from their inclusion as it learns to distinguish between dollar spots and other objects often present in fields of turfgrass. The dataset is partitioned into distinct subsets, allocating 80% for training, 10% for validation, and 10% for testing. Post data augmentation, this distribution resulted in a total of $11,830 \times 256 \times 256$ image samples for training, 1478 for testing, and 1478 for validation.

The dollar spot images also ranged in season and genera, including both warm- and cool-season turfgrasses, including fescues (*Festuca* spp. L.), creeping bentgrass (*Agrostis stolonifera*), bermudagrass (*Cynodon dactylon*), and zoysiagrass (*Zoysia japonica*). Images also included a wide range of turfgrass heights of cut, including golf course greens (3 mm) and fairway height (8–15 mm), in addition to taller lawn heights (5–8 cm).

Because these images were taken during trials, many show disease progressing within plots, from visibly ambiguous amounts of dollar spot to plots where large portions of the turfgrass have died. Incorporating images from various seasons, turfgrass species, and disease stages enriches the training dataset, improving the model's ability to accurately identify and quantify dollar spot under a wide array of conditions. Training with seasonal variation teaches the model to adjust for differences in lighting and color variations, which is essential for year-round disease detection. Including diverse turfgrass species, heights of cut, and disease stages broadens the model's diagnostic scope, increasing its utility across different cultivars and stages of disease progression. Such dataset diversity is needed to fine-tune a model to perform well across the multifaceted scenarios encountered in practical applications (Sladojevic et al., 2016).

Every visible instance of dollar spot within the training dataset was manually segmented by a trained turfgrass pathologist until every image had a corresponding mask. Every mask was then reviewed by a separate person to double-check its accuracy. To augment the dataset and enhance the robustness of the model, each image and corresponding mask was sliced into nonoverlapping 256×256 pixel tiles. Slicing the images into smaller sections allows the model to focus on localized features of the disease, which is particularly beneficial for learning to identify and quantify smaller or early-stage disease manifestations (Perez & Wang, 2017). Subsequently, each tile is augmented through horizontal flipping to create mirror images. Mirroring images adds variability by presenting the model with flipped versions of the images. This forces it to learn disease features regardless of their orientation, which improves the model's ability to generalize from the training data to new, unseen images (Shorten & Khoshgoftaar,

2019). These augmentation techniques are used to artificially expand the dataset, providing a more diverse set of training examples (Figure 2). Data augmentation not only helps to mitigate overfitting but also enhances the generalization capacity of deep learning algorithms by exposing them to variations that simulate potential transformations in real-world scenarios (Taylor & Nitschke, 2018).

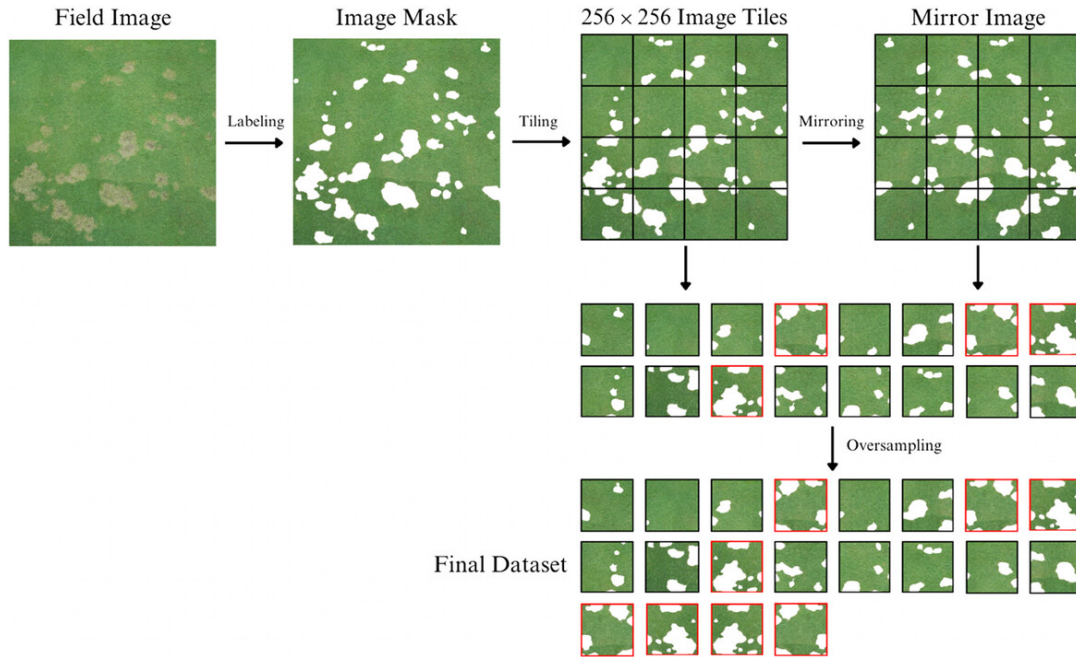


Figure 2: Data preprocessing and augmentation from left to right: every instance of dollar spot from the original field image of dollar spot is labeled by hand to create the mask. The mask is then sliced into 256×256 pixel tiles and a mirror image is generated. The tiles from the image and its mirror are both added to the dataset, and any tiles with more than 20% disease are duplicated in the final dataset.

To further assess the model's robustness across varying levels of disease manifestation, the images were stratified into three classes based on the prevalence of dollar spot. Images exhibiting disease coverage between 20% and 100%, totaling 848 images; those

with coverage ranging from 5% to 20%, totaling 2368 images; and images with less than 5% disease coverage, totaling 8614 images. This stratification facilitates a more nuanced evaluation of the model's performance across different levels of disease severity.

Oversampling was applied to the minority class by duplicating training images with 20%–100% disease coverage. While this helps minimize the class imbalance within the dataset by increasing the total amount of dollar spot the model sees in each epoch, it does not significantly contribute to overfitting because the number of easy images is small relative to the rest of the training dataset. Oversampling alone does not adequately address the class imbalance, however, as the amount of diseased turf is naturally sparse compared with the amount of asymptomatic grass in most images.

DeepLab3V+ is pretrained on ImageNet (Stanford Vision Lab), a database containing over 14 million high-resolution images categorized into thousands of classes (Deng et al., 2009). Pretraining with ImageNet does not significantly affect the model's accuracy or precision in segmenting instances of dollar spot; rather, it helps the model converge faster and enhances its ability to accurately distinguish nontarget class objects. At the outset of the study, it was observed that using pretrained weights initially hindered the model's convergence. This was likely due to our limited training data being insufficient to override the biases the model learned from pretraining on ImageNet's extensive and diverse dataset. To address this, the dataset was expanded by doubling the number of labeled images and implementing the aforementioned data augmentation techniques.

In order to train the model to differentiate dollar spot from other turfgrass diseases and to prevent false positives on nontarget objects that the model could mistake for dollar

spot, the dataset included 1164 negative images. The negative images included the diseases brown patch (*Rhizoctonia solani*), spring dead spot (*Ophiosphaerella* spp.), summer patch (*Magnaportheopsis* spp.), and grey leaf spot (*Pyricularia grisea*). Negative images also included abiotic factors and items, such as drought stress, scalping, patches of soil or sand, golf balls, and divots.

2.3 Encoder and decoder

ResNet-34 was selected as the encoder for our model primarily due to its relatively small memory footprint, which facilitates efficient training and testing on the computer used in this study (Table 1). In contrast, while a deeper network such as ResNet-152 could potentially capture a more extensive range of features from the input images, its larger memory requirements exceed the capacity of our available computing resources (He et al., 2016).

Table 1. Specifications of computing environment used in this study for deep learning of dollar spot detection.

Component	Specification
Operating system	Ubuntu 22.04
GPU	NVIDIA T550 Laptop GPU
Cores	20
VRAM	3.81 GB
RAM	16 GB
CUDA version	12.2

PyTorch version	2.2.2
-----------------	-------

Abbreviation: GPU, graphics processing unit.

In the context of deep learning, an encoder is a critical component of a neural network that compresses input data into a more compact representation. Specifically, ResNet-34, a convolutional neural network processes an image to produce a feature vector that encapsulates the essential characteristics of the input, making it suitable for subsequent prediction tasks. The architecture of ResNet-34 uses fewer layers than ResNet-152, which not only reduces the memory demands but also suffices for capturing the necessary features for effective segmentation (He et al., 2016).

The decoder component of a neural network expands latent representations back to higher dimensional spaces suitable for specific tasks like classification or segmentation. In our model, the decoder module enhances the segmentation accuracy along dollar spot boundaries, ensuring precise delineation of the targeted regions (Chen et al., 2018).

2.4 Loss calculation

The dataset used for this project exhibited an inherent class imbalance due to the outsized prevalence of asymptomatic turfgrass compared with dollar spot-infested turfgrass in most images. Without adjusting the loss function, the model learns to optimize its performance by consistently predicting the dominant class. Loss in neural networks quantifies the difference between the predicted values and the actual values. This guides the network during the training phase toward more accurate predictions as it attempts to minimize loss. The task of segmenting areas of dollar spot disease in a turfgrass canopy is a binary classification problem because there are only two classes: “dollar spot” and

“non-dollar spot.” Every pixel of the input images is scrutinized for the probability that it indicates dollar spot disease or not. To account for the class imbalance, we used a weighted binary cross-entropy loss function. This function modifies the standard binary cross-entropy loss by introducing class-specific weights, which can help balance the influence of each class on the model's learning process (Lin et al., 2017). The weights are adjusted to amplify the penalty for incorrectly classifying the less represented class (turfgrass with dollar spot), thereby mitigating the bias toward the dominant class (turfgrass without dollar spot). This adjustment enables the model to learn a more balanced representation of both classes.

2.5 Training and validation

To train DeepLabV3+, we used a ResNet-34 CNN encoder pre-initialized with ImageNet weights and the AdamW optimizer with an initial learning rate of 0.0005. The learning rate was adjusted based on the model's performance during validation, and we used a weighted binary cross-entropy loss function to manage class imbalance. Training was conducted over eight epochs in batches of eight images and was completed in under 3 h. All training took place on an NVIDIA T550 Laptop graphics processing unit (GPU) with PyTorch 2.2.2 and CUDA 12.2 (Table 1), with periodic evaluations of intersection over union (IoU) and F1 scores to fine-tune the threshold for classification. During validation, the model was evaluated across various confidence thresholds to determine the optimal setting by comparing the resulting IoU and F1 scores. Figure 3 illustrates the implications of various confidence thresholds. The 10% threshold is too lenient, as even uncertain predictions are included in the predicted mask. In this case, the model

erroneously predicted that the lightly colored pixels on the leaf indicate dollar spot. Conversely, the 99% confidence threshold is excessively stringent, such that even the model's most confident and accurate predictions fail to qualify. The 90% threshold is optimal since the probabilities the model has produced to indicate the likelihood of dollar spot infestation for each pixel are accurately reflected in the predicted mask.

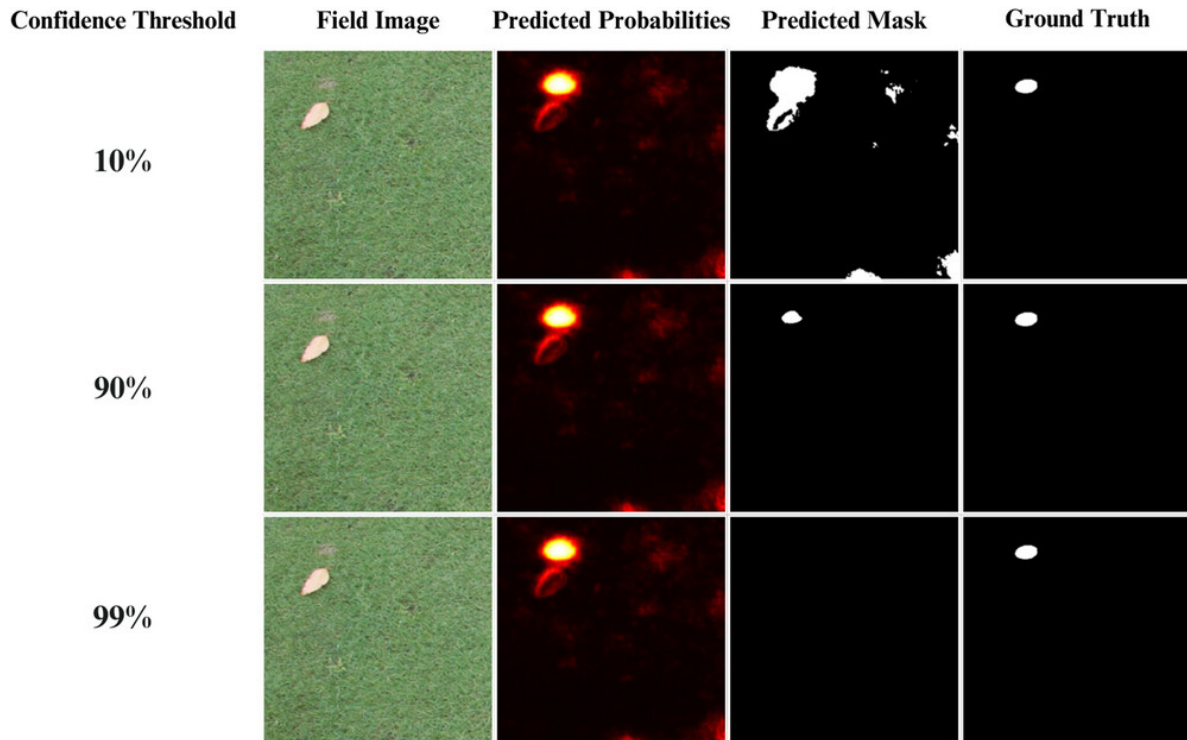


Figure 3: Predicted dollar spot masks from a creeping bentgrass fairway using varying confidence thresholds. Columns from left to right represent the original image, the predicted probability, the predicted mask, and the ground truth image used for training. Rows represent dollar spot predictions at confidence thresholds of 10%, 90%, and 99%.

2.6 Performance metrics

To assess the performance of the trained model, we computed several standard metrics, each offering a unique perspective on the model's effectiveness:

1. F1 Score: This metric is the harmonic mean of precision and recall, providing a balanced measure of the model's accuracy and completeness in identifying dollar spot-affected areas.

$$F1 = 2 \times \frac{\text{Precision} \times \text{Recall}}{\text{Precision} + \text{Recall}}$$

$$\text{Where precision} = \frac{TP}{TP + FP} \text{ and recall} = \frac{TP}{TP + FN}$$

Here, TP is the number of true positives, FP is the number of false positives, and FN is the number of false negatives. The F1 score provides a balanced measure of the model's precision and recall

2. Mean Intersection over Union (Mean IoU): This metric quantifies the overlap between the predicted segmentation and the actual ground truth, offering a precise measure of the model's segmentation accuracy.

$$IoU = \frac{TP}{TP + FN + FP}$$

$$mIoU = \frac{1}{C} \sum_{i=1}^C IoU_i$$

Where C is the total number of classes, TP is the number of true positives, FN is the number of false negatives, and FP is the number of false positives for each class. The mIoU measures the average overlap between the predicted and ground truth segments for all classes. For our binary classification task, C = 2.

3. Mean Pixel Accuracy: This metric measures the average accuracy of all pixels across all images.

$$\text{MPA} = \frac{1}{N} \sum_{i=1}^N 1(y_i = \hat{y}_i)$$

Where N is the total number of pixels, y_i is the ground truth label of the i th pixel, \hat{y}_i is the predicted label of the i th pixel, and $1(y_i = \hat{y}_i)$ is an indicator function that equals 1 if $y_i = \hat{y}_i$ and 0 otherwise. This metric measures the average accuracy of all pixels across all images.

4. Mean Accuracy: This metric measures the average accuracy per image in a batch by calculating the accuracy for each image and averaging these accuracies.

$$\text{MA} = \frac{1}{C} \times \sum_{i=1}^C \frac{\text{TP}_i}{\text{TP}_i + \text{FN}_i}$$

Where C is the total number of classes, TP is the number of true positives for each class, and FN is the number of false negatives for each class. Mean accuracy measures the average accuracy per image in a batch by calculating the accuracy for each image and averaging these accuracies. For our binary classification task, $C = 2$.

These calculations provide a comprehensive assessment of semantic segmentation model performance (Thoma, 2016; Csurka et al., 2023) and validate whether fine-tuning to distinguish and segment dollar spot-affected areas of turfgrass has succeeded.

Results

Overall, the model achieved a mean pixel accuracy of .97, a mean accuracy of .89, a mean IoU of .72, and a mean F1 score of .74. Table 2 displays the performance of

the model across three disease prevalence levels. The model was able to identify and segment instances of disease with an average inference time of 6 ms per image.

Table 2: Performance metrics across varying levels of disease prevalence.

Disease Prevalence	0-5% Disease	5%-20% Disease	20%-100% Disease
Mean F1 Score	0.6928	0.76188	0.7318
Mean IoU	0.7064	0.6319	0.5797
Mean Pixel Accuracy	0.9884	0.9365	0.7722
Mean Accuracy	0.8748	0.9008	0.8059

Discussion

The model demonstrated better performance on images of closely mown turfgrass compared to taller, lawn-height grasses. This can be attributed to the more discrete edges of dollar spot infection centers on shorter grass, which appear as small circles (<50 mm) in contrast to the larger, irregular patches observed on taller grass (Tredway et al., 2022). Despite being trained on a diverse dataset that included both grass heights, the model showed greater precision in identifying the clearer infection patterns of shorter turf. To address this, future enhancements could focus on improving the model’s sensitivity to the subtler and more irregular visual cues of dollar spot in taller grass, potentially through targeted algorithmic adjustments that enhance feature detection in these less distinct patterns.

The model also tends to learn color contrast as an important feature of its predictions. This is an important feature for the model to learn, since most instances of

dollar spot are characterized by tan or off-white spots dotting a green surface. However, the model's reliance on contrast becomes a limitation under certain conditions. When the contrast between the diseased spots and the surrounding grass is subdued—due to either the natural color of the grass or external lighting—the model's predictive accuracy is diminished.

The performance of the model is ultimately limited by the quantity, diversity, and accuracy of the labels the model is trained on. Fine-tuning a model to effectively segment turfgrass disease requires a considerable time investment to collect a diverse set of disease samples and precisely annotate them. However, this initial period of inefficiency will enable practitioners to receive accurate and consistent predictions within milliseconds in the future.

The promising results of applying DeepLabV3+ for dollar spot detection and quantification in turfgrass highlight the potential to leverage deep learning in agricultural and environmental monitoring more broadly. Given the success of this model in accurately identifying and quantifying dollar spot severity, similar methodologies could be applied to a wider range of turfgrass diseases and other pests. Future studies could explore the adaptability of this model to other turfgrass conditions, such as drought stress or damage from physical wear, which are also critical to maintaining the health and aesthetic value of turfgrass landscapes.

However, there is ample room for improvements and broader applications of this model. Further studies should focus on extending the model's utility across various diseases, weeds, or other turfgrass afflictions. To quantify the model's ability to differentiate between dollar spot and other turfgrass pests and afflictions, a confusion

matrix should be conducted to analyze the model's performance. Integrating advanced imaging techniques, such as high-resolution multispectral and hyperspectral imagery from drones, satellites, and equipment-mounted sensors, could significantly refine the model's detection capabilities by providing detailed insights into plant health invisible to the naked eye (Zhang & Kovacs, 2012). Additionally, developing real-time disease monitoring systems using Internet of Things, or IoT, devices could improve disease management by enabling immediate identification and treatment actions (Liakos et al., 2018).

The practical implications of automating disease detection can also significantly streamline the labor-intensive process of monitoring disease spread. Traditionally, this has involved manually counting new infection centers or visually quantifying the percent disease coverage, a method detailed in studies by Smith et al., 2018; Steketee et al., 2016, Ryan et al., 2012. By using models like DeepLabV3+, which automates and accurately quantifies infection centers, the precision of treatments can be enhanced. This allows for interventions that are more tailored to the specific severity and spread of infections as detected by these advanced technologies. Such automation could greatly improve the efficiency and accuracy of disease management processes in turf management.

The objective of this study was to fine-tune and evaluate a deep learning semantic segmentation model capable of accurately identifying and quantifying the severity of dollar spot disease in turfgrass. These results demonstrate that a pre-trained deep learning model, fine-tuned on a small set of expert-labeled images and trained on a personal computer, can achieve significant accuracy and precision in segmenting instances of dollar spot in turfgrass. It shows that large teams of developers, advanced GPUs, and

extensive computational resources are not necessary to obtain high-quality segmentation results when leveraging advanced pre-trained models developed through the dedicated efforts of preceding researchers. This approach enables turfgrass scientists and professionals to objectively quantify the severity of dollar spot infections more efficiently and accurately than traditional methods, which are often time-consuming and subjective.

By providing a reliable, accessible tool for disease assessment, this work enables the adoption of similar methodologies for other turfgrass diseases, broadening the scope of disease management and potentially transforming practices in the field. This validation supports further research into the use of deep learning models to perform time-intensive, subjective visual assessments for disease analysis in turfgrass pathology and motivates the development of more accessible and efficient disease management strategies.

Bibliography

1. Barnes, M. R., Nelson, K. C., & Dahmus, M. E. (2020). What's in a yardscape? A case study of emergent ecosystem services and disservices within resident yardscape discourses in Minnesota. *Urban Ecosystems*, 23, 1167–1179.
2. Beard, J. B., & Green, R. L. (1994). The Role of Turfgrasses in Environmental Protection and Their Benefits to Humans. *Journal of Environmental Quality*, 23(3), 452–460. <https://doi.org/10.2134/jeq1994.00472425002300030007x>
3. Bock, C. H., Barbedo, J. G., Del Ponte, E. M., Bohnenkamp, D., & Mahlein, A.-K. (2020). From visual estimates to fully automated sensor-based measurements of plant disease severity: Status and challenges for improving accuracy. *Phytopathology Research*, 2, 1–30.
4. Boulent, J., Foucher, S., Théau, J., & St-Charles, P.-L. (2019). Convolutional Neural Networks for the Automatic Identification of Plant Diseases. *Frontiers in Plant Science*, 10, 941. <https://doi.org/10.3389/fpls.2019.00941>
5. Chen, L.-C., Zhu, Y., Papandreou, G., Schroff, F., & Adam, H. (2018). Encoder-Decoder with Atrous Separable Convolution for Semantic Image Segmentation. <https://doi.org/10.48550/ARXIV.1802.02611>
6. Csurka, G., Volpi, R., & Chidlovskii, B. (2023). Semantic Image Segmentation: Two Decades of Research. <https://doi.org/10.48550/ARXIV.2302.06378>
7. Deng, J., Dong, W., Socher, R., Li, L.-J., Kai Li, & Li Fei-Fei. (2009). ImageNet: A large-scale hierarchical image database. 2009 IEEE Conference on Computer Vision and Pattern Recognition, 248–255. <https://doi.org/10.1109/CVPR.2009.5206848>
8. Durmus, H., Gunes, E. O., & Kirci, M. (2017). Disease detection on the leaves of the tomato plants by using deep learning. 2017 6th International Conference on Agro-Geoinformatics, 1–5. <https://doi.org/10.1109/Agro-Geoinformatics.2017.8047016>
9. Garcia-Garcia, A., Orts-Escolano, S., Oprea, S., Villena-Martinez, V., & Garcia-Rodriguez, J. (2017). A Review on Deep Learning Techniques Applied to Semantic Segmentation. <https://doi.org/10.48550/ARXIV.1704.06857>
10. Goodman, D. M., & Burpee, L. L. (1991). Biological control of dollar spot disease of creeping bentgrass. *Phytopathology*, 81(11), 1438–1446.
11. Hasan, R. I., Yusuf, S. M., & Alzubaidi, L. (2020). Review of the State of the Art of Deep Learning for Plant Diseases: A Broad Analysis and Discussion. *Plants*, 9(10), 1302. <https://doi.org/10.3390/plants9101302>
12. He, K., Zhang, X., Ren, S., & Sun, J. (2016). Deep residual learning for image recognition. *Proceedings of the IEEE Conference on Computer Vision and Pattern Recognition*, 770–778.

13. Jung, H., & Chung, C. (2024). Consumers' WTP for Sustainability Turfgrass Attributes with Consideration of Aesthetic Attributes and Water Conservation Policies. *Agriculture*, 14(1), 159.
14. Krenitsky, E. C., Carroll, M. J., Hill, R. L., & Krouse, J. M. (1998). Runoff and sediment losses from natural and man-made erosion control materials. *Crop Science*, 38(4), 1042–1046.
15. Liakos, K. G., Busato, P., Moshou, D., Pearson, S., & Bochtis, D. (2018). Machine learning in agriculture: A review. *Sensors*, 18(8), 2674.
16. Lin, T.-Y., Goyal, P., Girshick, R., He, K., & Dollár, P. (2017). Focal loss for dense object detection. *Proceedings of the IEEE International Conference on Computer Vision*, 2980–2988.
17. Liu, J., & Wang, X. (2021). Plant diseases and pests detection based on deep learning: A review. *Plant Methods*, 17(1), 22. <https://doi.org/10.1186/s13007-021-00722-9>
18. Miao, C., Pages, A., Xu, Z., Rodene, E., Yang, J., & Schnable, J. C. (2020). Semantic Segmentation of Sorghum Using Hyperspectral Data Identifies Genetic Associations. *Plant Phenomics*, 2020, 2020/4216373. <https://doi.org/10.34133/2020/4216373>
19. Milesi, C., Running, S. W., Elvidge, C. D., Dietz, J. B., Tuttle, B. T., & Nemani, R. R. (2005). Mapping and modeling the biogeochemical cycling of turf grasses in the United States. *Environmental Management*, 36, 426–438.
20. Monteiro, J. A. (2017). Ecosystem services from turfgrass landscapes. *Urban Forestry & Urban Greening*, 26, 151–157.
21. Nutter Jr, F. W., Gleason, M. L., Jenco, J. H., & Christians, N. C. (1993). Assessing the accuracy, intra-rater repeatability, and inter-rater reliability of disease assessment systems. *Phytopathology*, 83(8), 806–812.
22. Perez, L., & Wang, J. (2017). The effectiveness of data augmentation in image classification using deep learning. *arXiv Preprint arXiv:1712.04621*.
23. Peters, E. B., Hiller, R. V., & McFadden, J. P. (2011). Seasonal contributions of vegetation types to suburban evapotranspiration. *Journal of Geophysical Research: Biogeosciences*, 116(G1).
24. Ryan, C. P., Dernoeden, P. H., & Grybauskas, A. P. (2012). Seasonal Development of Dollar Spot Epidemics in Six Creeping Bentgrass Cultivars in Maryland. *HortScience*, 47(3), 422–426. <https://doi.org/10.21273/HORTSCI.47.3.422>
25. Salgado-Salazar, C., Beirn, L. A., Ismaiel, A., Boehm, M. J., Carbone, I., Putman, A. I., Tredway, L. P., Clarke, B. B., & Crouch, J. A. (2018). *Clarireedia*: A new fungal genus

26. comprising four pathogenic species responsible for dollar spot disease of turfgrass. *Fungal Biology*, 122(8), 761–773.
<https://doi.org/10.1016/j.funbio.2018.04.004>
27. Sapkota, S., Catching, K. E., Raymer, P. L., Martinez-Espinoza, A. D., & Bahri, B. A. (2022). New Approaches to an Old Problem: Dollar Spot of Turfgrass. *Phytopathology*®, 112(3), 469–480. <https://doi.org/10.1094/PHYTO-11-20-0505-RVW>
28. Schwanck, A. A., & Del Ponte, E. M. (2014). Accuracy and reliability of severity estimates using linear or logarithmic disease diagram sets in true colour or black and white: A study case for rice brown spot. *Journal of Phytopathology*, 162(10), 670–682.
29. Shahi, T. B., Xu, C.-Y., Neupane, A., & Guo, W. (2023). Recent Advances in Crop Disease Detection Using UAV and Deep Learning Techniques. *Remote Sensing*, 15(9), 2450. <https://doi.org/10.3390/rs15092450>
30. Shorten, C., & Khoshgoftaar, T. M. (2019). A survey on image data augmentation for deep learning. *Journal of Big Data*, 6(1), 1–48.
31. Sladojevic, S., Arsenovic, M., Anderla, A., Culibrk, D., & Stefanovic, D. (2016). Deep neural networks based recognition of plant diseases by leaf image classification. *Computational Intelligence and Neuroscience*, 2016.
32. Smith, D. L., Kerns, J. P., Walker, N. R., Payne, A. F., Horvath, B., Inguagiato, J. C., Kaminski, J. E., Tomaso-Peterson, M., & Koch, P. L. (2018). Development and validation of a weather-based warning system to advise fungicide applications to control dollar spot on turfgrass. *PLOS ONE*, 13(3), e0194216.
<https://doi.org/10.1371/journal.pone.0194216>
33. Steketee, C. J., Martinez-Espinoza, A. D., Harris-Shultz, K. R., Henry, G. M., & Raymer, P. L. (2016). Effects of Genotype and Isolate on Expression of Dollar Spot in Seashore Paspalum. *HortScience*, 51(1), 67–73.
<https://doi.org/10.21273/HORTSCI.51.1.67>
34. Stier, J. C., Steinke, K., Ervin, E. H., Higginson, F. R., & McMaugh, P. E. (2015). Turfgrass Benefits and Issues. In J. C. Stier, B. P. Horgan, & S. A. Bonos (Eds.), *Turfgrass: Biology, Use, and Management* (pp. 105–145). American Society of Agronomy, Crop Science Society of America, Soil Science Society of America. <https://doi.org/10.2134/agronmonogr56.c3>
35. Taylor, L., & Nitschke, G. (2018). Improving deep learning with generic data augmentation. 2018 IEEE Symposium Series on Computational Intelligence (SSCI), 1542–1547.
36. Thoma, M. (2016). A Survey of Semantic Segmentation.
<https://doi.org/10.48550/ARXIV.1602.06541>
37. Thomas, S., Behmann, J., Steier, A., Kraska, T., Muller, O., Rascher, U., & Mahlein, A.-K. (2018). Quantitative assessment of disease severity and rating of

- barley cultivars based on hyperspectral imaging in a non-invasive, automated phenotyping platform. *Plant Methods*, 14, 1–12.
38. Tredway, L. P., Clarke, B. B., Kerns, J. P., & Tomaso-Peterson, M. (Eds.). (2022). *Compendium of Turfgrass diseases (Fourth edition)*. The American Phytopathological Society.
 39. Vargas, J. M. (2018). *Management of Turfgrass Diseases (2nd ed.)*. CRC Press. <https://doi.org/10.1201/9780203748374>
 40. Waldamichael, F. G., Debelee, T. G., Schwenker, F., Ayano, Y. M., & Kebede, S. R. (2022). Machine Learning in Cereal Crops Disease Detection: A Review. *Algorithms*, 15(3), 75. <https://doi.org/10.3390/a15030075>
 41. Walsh, B., Ikeda, S. S., & Boland, G. J. (1999). Biology and management of dollar spot (*Sclerotinia homoeocarpa*); an important disease of turfgrass. *HortScience*, 34(1), 13–21.
 42. Wang, X. (2016). Deep Learning in Object Recognition, Detection, and Segmentation. *Foundations and Trends® in Signal Processing*, 8(4), 217–382. <https://doi.org/10.1561/20000000071>
 43. Yu, J., Sharpe, S. M., Schumann, A. W., & Boyd, N. S. (2019). Deep learning for image-based weed detection in turfgrass. *European Journal of Agronomy*, 104, 78–84. <https://doi.org/10.1016/j.eja.2019.01.004>
 44. Yu, M., Ma, X., Guan, H., Liu, M., & Zhang, T. (2022). A Recognition Method of Soybean Leaf Diseases Based on an Improved Deep Learning Model. *Frontiers in Plant Science*, 13, 878834. <https://doi.org/10.3389/fpls.2022.878834>
 45. Yue, C., Cui, M., Watkins, E., & Patton, A. (2021). Investigating factors influencing consumer adoption of low-input turfgrasses. *HortScience*, 56(10), 1213–1220.
 46. Zhang, C., & Kovacs, J. M. (2012). The application of small unmanned aerial systems for precision agriculture: A review. *Precision Agriculture*, 13, 693–712.
 47. Zhou, Q., & Soldat, D. J. (2021). Creeping Bentgrass Yield Prediction With Machine Learning Models. *Frontiers in Plant Science*, 12, 749854. <https://doi.org/10.3389/fpls.2021.749854>